

# Asymptotic generalization error of a single-layer graph convolutional network

Odilon Duranthon and Lenka Zdeborová

Statistical Physics of Computation laboratory,

École polytechnique fédérale de Lausanne (EPFL), Switzerland

`firstname.lastname@epfl.ch`

## Abstract

While graph convolutional networks show great practical promises, the theoretical understanding of their generalization properties as a function of the number of samples is still in its infancy compared to the more broadly studied case of supervised fully connected neural networks. In this article, we predict the performances of a single-layer graph convolutional network (GCN) trained on data produced by attributed stochastic block models (SBMs) in the high-dimensional limit. Previously, only ridge regression on contextual-SBM (CSBM) has been considered in [21]; we generalize the analysis to arbitrary convex loss and regularization for the CSBM and add the analysis for another data model, the neural-prior SBM. We also study the high signal-to-noise ratio limit, detail the convergence rates of the GCN and show that, while consistent, it does not reach the Bayes-optimal rate for any of the considered cases.

## 1 Introduction

Understanding the generalization properties of neural networks, in general, is still unsatisfactory despite the very active line of work in this direction. In this article, we are specifically interested in understanding the generalization properties of *graph* neural networks where the question remains even further from closed compared to feedforward neural networks that have been explored in the theoretical literature more broadly.

The question of generalization has been studied from many angles. Classical learning theory usually aims to avoid assumptions on the data distribution and to provide generic generalization bounds. Such bounds are, however, often far away from the actual performance on given benchmark datasets, see e.g. [24]. This generic line of work is hence complemented by studies of concrete data distributions and concrete target functions for which a tight (i.e. including the constants) high-dimensional analysis is possible; for examples, see e.g. [5, 17, 19]. In those cases one can evaluate the gap between the generalization ability of neural networks and the information-theoretically optimal generalization (that is often also analyzable in the same settings). If such a comparison were possible for state-of-the-art neural network architectures, then the amplitude of the gaps to optimality could be used to drive the development of architectures that decrease the gap. So far this is not the case; the tight asymptotic analysis was established only for very simple architectures, e.g. single layer and two-layer neural networks; and there are still many open questions even for the two-layer case. However, the long-term promise of this line of work drives efforts to establish the tight asymptotic analysis is broader and broader settings. The present work is inscribed in this context.

Graph neural networks show a broad range of practical applications and as such understanding their generalization properties is an important part of the overall goal. Many works consider graph or node classification in a learning scenario where one has access to many training graphs and unseen test graphs. Some works then derive bounds based on VC dimension, Rademacher complexity or PAC-Bayesian analysis, see for instance [13] and the references therein. We instead consider the semi-supervised (or transductive) learning scenario, where training and inference are done on the same large graph whose node labels are partially revealed. This setting is relevant for node classification problems such as community detection. Previous theoretical works on semi-supervised learning include [22], that studies learning under stochastic gradient descent, or [7] that focuses on graph convolutional networks (GCN) and proposes experiments on data generated by the contextual stochastic block model (CSBM). More similar questions as our work are

addressed in [11] that derives generalization bounds for a particular model of data close to the CSBM; yet it considers a generic GNN and the bounds are not tight.

A series of works closer to our article has been developed by the authors of [3]. In this work they consider a one-layer GCN trained on the CSBM by logistic regression and derive bounds for the test loss; however, they analyze its generalization ability on new graphs that are independent of the train graph and do not give exact predictions. In [4] they propose an architecture of GNN that is optimal for the CSBM, among classifiers that process local tree-like neighborhoods, and they exactly derive its generalization error. These two works consider a low-dimensional setting.

The tight analysis of generalization in synthetic high-dimensional setting for GNNs is in its infancy. The only pioneering reference in this direction we are aware of is [21] where the authors consider a simple one-layer graph convolutional network (GCN) trained in a semi-supervised way by ridge regression. They predict its asymptotic performances on data generated by the contextual stochastic block model (CSBM) and in particular show how to tune the architecture to adapt to the homophily strength of the graph.

A starting point of the tight asymptotic analysis of generalization is a suitable model for generating data. As [21] showed, the CSBM introduced in [23, 8] is suitable. Data generated by this model has been used to benchmark various GNN architectures in [6, 7, 12, 14] for instance. Another way to generate graph data with node features is the neural-prior SBM and the generalized linear model SBM (GLM–SBM) introduced in [9], where the features alone do not bring any information. For these two models, the CSBM and the GLM–SBM, the optimal performances has been derived in the high-dimensional limit in [10, 2, 9].

We are inspired by the work of [21] where the learning of a GCN with regularized square loss is analyzed but not compared to the Bayes-optimal performance. Our motivations to extend this work comes from the related line of work on tight high-dimensional asymptotic on the feedforward supervised setting [1, 18] that established that the generalization error of the ridge regression is suboptimal for some models of data while the one of logistic regression is much closer to Bayes-optimal. When it comes to rates with which the test error goes to zero in the limit of a large number of samples, they are again suboptimal for ridge regression while they give the Bayes-optimal rates for optimally regularized logistic regression [1]. For a slightly different setting the Bayes-optimal performance can be achieved [18] just by adjusting the regularization. Natural questions thus are: how does the performance of the GCN from [21] compare to the Bayes-optimal performance? How much does optimal regularization or more suitable loss improve the generalization? How does this reflect in rates when the signal-to-noise ratio is large? These questions are answered in the present work.

**Main contribution:** In the first part, we generalize the analysis of [21] by considering generic loss and regularization for the CSBM and the GLM–SBM. We derive and state the closed-form equations predicting the generalization performance of the GCN in the high-dimensional limit. We compare to the Bayes-optimal test accuracy, search for the optimal parameters of the considered architecture, and explore several common loss functions. We show that in the considered setting large regularization maximizes the test accuracy; ridge regression has a large gap to the optimality, and the logistic and hinge losses do not improve it significantly. This stands for both the considered models and is thus different from the single layer perceptron learning from data generated by the teacher-student model of [1].

In the second part, we consider the limit of high signal-to-noise ratio (snr). We show that the simple GCN we consider is consistent in the sense that the test error converges to zero as the snr diverges. We derive the convergence rates for the two models. In all cases we investigated the rates are smaller than the Bayes-optimal one which is again in disparity with the well-studied feed-forward case [1].

## 2 Models, setup

**Attributed SBMs:** We consider set of  $N$  nodes and a graph  $G$ . Each node  $i$  has a label  $y_i = \pm 1$ ; we consider two balanced groups. We precise the law of  $y_i$  later. We observe an adjacency matrix  $A \in \mathbb{R}^{N \times N}$  drawn according to

$$A_{ij} = \mathcal{B} \left( \frac{d}{N} + \frac{\lambda}{\sqrt{N}} \sqrt{\frac{d}{N} \left( 1 - \frac{d}{N} \right)} y_i y_j \right) \quad (1)$$

where  $\lambda$  is the signal-to-noise ratio (snr) of the graph,  $d$  is the average degree of the graph and the components  $A_{ij}$  are independant Bernoulli variables. We take an average degree  $d$  of order  $N$ , but  $d$  growing with  $N$  should be sufficient for our results to hold. We consider a directed SBM,  $A$  non-symmetric, to simplify the analysis. This model can be mapped to a non-directed SBM of snr  $\lambda' = \sqrt{2}\lambda$  by taking the adjacency matrix  $(A + A^T)/\sqrt{2}$ .

We consider  $M$  hidden variables  $u_\nu \sim \mathcal{N}(0, 1)$ ; we set  $\alpha = N/M$  the aspect ratio. We also observe features  $X \in \mathbb{R}^{N \times M}$ . The features are correlated with the node labels. We consider first the contextual stochastic block model (CSBM) [23, 8] for which the labels are Rademacher and the features follow a Gaussian mixture:

$$(\text{CSBM}) \quad y_i \sim \text{Rad} , \quad X = \sqrt{\frac{\mu}{N}} y u^T + W \quad (2)$$

where  $\mu$  is the snr of the features and  $W$  is noise whose components  $W_{i\nu}$  are independent standard Gaussians. The total snr of the symmetric CSBM is [8]

$$\text{snr}_{\text{CSBM}} = \lambda^2 + \frac{\mu^2}{\alpha} . \quad (3)$$

Authors of [8, 16] showed that  $\text{snr}_{\text{CSBM}} = 1$  is the detectability threshold in the sense that in the unsupervised case it separates a undetectable phase, where the labels cannot be recovered better than at random, from a detectable phase where they can. The expression shows that the snr originating from the graph is of the strength  $\lambda^2$  while the one originating from the features is  $\frac{\mu^2}{\alpha}$ .

We will also consider another related model, the GLM-SBM [9], for which the features are Gaussian and the labels are generated by a generalized linear model (GLM) on the features:

$$(\text{GLM-SBM}) \quad X_{i\nu} \sim \mathcal{N}(0, 1) , \quad y = \text{sign} \left( \frac{1}{\sqrt{N}} X u \right) \quad (4)$$

where  $\text{sign}$  is applied element-wise. The total snr of the symmetric GLM-SBM is

$$\text{snr}_{\text{GLM-SBM}} = \lambda^2 \left( 1 + \frac{4\alpha}{\pi^2} \right) . \quad (5)$$

Again in the unsupervised setting [9] established that  $\text{snr}_{\text{GLM-SBM}} = 1$  is the detectability threshold.

We are given a set  $R$  of train nodes and define  $\rho = |R|/N$  the training ratio. The test set  $R'$  is selected from the complement of  $R$ ; we define  $\rho' = |R'|/N$  the testing ratio. We assume that  $R$  and  $R'$  are independent from the other quantities. We precise that in the unsupervised case  $\rho = 0$  these two models admit a transition at  $\text{snr}_{\text{CSBM}}$  and  $\text{snr}_{\text{GLM-SBM}}$  equal 1, below which no information on the labels  $y$  can be recovered; while in the semi-supervised case  $\rho > 0$  this transition disappears and one can always recover some information on the test labels.

We work in a high-dimensional limit  $N \rightarrow \infty$  and  $M \rightarrow \infty$  while the aspect ratio  $\alpha = N/M$  being of order one. The other parameters  $\lambda$ ,  $\mu$ ,  $\rho$  and  $\rho'$  are also of order one.

The inference problem is to find back  $y$  and  $u$  given  $A$ ,  $X$ ,  $R$  and the parameters of the model. We study the performances of a graph neural network on this problem.

**Analyzed GCN architecture:** We follow [21] and we consider a single-layer graph convolutional network (GCN). It transforms the features according to

$$h(w) = \frac{1}{N} P(\tilde{A}) X w \quad (6)$$

where  $P$  is a polynomial,  $w \in \mathbb{R}^M$  are the trainable weights and  $\tilde{A} \in \mathbb{R}^{N \times N}$  is a rescaling of the adjacency matrix defined by

$$\tilde{A}_{ij} = \left( \frac{d}{N} \left( 1 - \frac{d}{N} \right) \right)^{-1/2} \left( A_{ij} - \frac{d}{N} \right) . \quad (7)$$

For the analysis, we consider  $P$  of degree one as in [21], i.e.  $P(\tilde{A}) = \tilde{A} + c\sqrt{N}I_N$  where  $c$  is a tunable parameter of the architecture. This corresponds to applying one step of graph convolution to the features with self-loops.

This GCN is trained by empirical risk minimization. We define the regularized loss

$$L_{A,X}(w) = \frac{1}{\rho N} \sum_{i \in R} l(y_i h_i(w)) + \frac{r}{\rho N} \sum_{\nu} \gamma(w_{\nu}) \quad (8)$$

where  $\gamma$  is a strictly convex regularization function,  $r$  is the regularization strength and  $l$  is a convex loss function. In the simulations we will focus on  $l_2$ -regularization  $\gamma(x) = x^2/2$  and on the square loss  $l(x) = (1-x)^2/2$ , the logistic loss  $l(x) = \log(1+e^{-x})$  or the hinge loss  $l(x) = \max(0, 1-x)$ . Since  $L$  is strictly convex it admits a unique minimizer  $w^*$ . The average train and test errors and accuracies of this model are

$$E_{\text{train/test}} = \mathbb{E} \frac{1}{|\hat{R}|} \sum_{i \in \hat{R}} l(y_i h(w^*)_i) \quad (9)$$

$$\text{Acc}_{\text{train/test}} = \mathbb{E} \frac{1}{|\hat{R}|} \sum_{i \in \hat{R}} \delta_{y_i = \text{sign } h(w^*)_i} \quad (10)$$

where  $\hat{R}$  stands either for the train set  $R$  or the test set  $R'$  and the expectation is taken over  $y, u, A, X, R$  and  $R'$ .

**Bayes-optimal performances:** The Bayes-optimal performance for both the CSBM and the GLM-SBM has been derived [10, 2]. They can be expressed as the fixed-point of a couple of scalar equations. These equations are reproduced in appendix B.

We will compare the performances of the GCN to the Bayes-optimal performances to see how large is the gap to optimality.

### 3 Main theoretical results

We compute the average errors and accuracies in the high-dimensional limit  $N$  and  $M$  large. This problem can be phrased in the same way as in [21]. We define the auxiliary loss function

$$H(w) = t \sum_{i \in R} l(y_i h(w)_i) + r \sum_{\nu} \gamma(w_{\nu}) + t' \sum_{i \in R'} l(y_i h(w)_i) \quad (11)$$

where  $t$  and  $t'$  are external parameters to give analytical access to the observables. The loss of the test samples is in  $H$  for the purpose of the analysis; we will take  $t' = 0$  later and the algorithm is still minimizing the training loss eq. 8. The moment generating function  $f$  (the free energy) is defined as

$$Z = \int dw e^{-\beta H(w)}, \quad f = -\frac{1}{\beta N} \mathbb{E} \log Z. \quad (12)$$

$\beta$  is an ancillary parameter to minimize the loss: we consider the limit  $\beta \rightarrow \infty$  where  $Z$  concentrates over  $w^*$  at  $t = 1$  and  $t' = 0$ . The train and test errors are then obtained according to

$$E_{\text{train}} = \frac{1}{\rho} \frac{\partial f}{\partial t}, \quad E_{\text{test}} = \frac{1}{\rho'} \frac{\partial f}{\partial t'} \quad (13)$$

both evaluated at  $t = 1$  and  $t' = 0$ . One can in the same manner compute the average accuracies by introducing the observables  $\sum_{i \in \hat{R}} \delta_{y_i = \text{sign } h(w)_i}$  in  $H$ .

To compute  $f$  we use the replica method, from Statistical Physics:

$$\mathbb{E} \log Z = \mathbb{E} \frac{\partial}{\partial n} Z^n(n=0) = \frac{\partial}{\partial n} \mathbb{E} Z^n(n=0). \quad (14)$$

$Z^n$  is interpreted as having  $n$  independent copies (replica) of the initial system, that become coupled by the expectation. We need to introduce an intermediate variable  $\sigma = \frac{1}{\sqrt{N}}Xw$ . We pursue the computation under the replica symmetry (RS) assumption. RS is justified by the convexity of  $H$ .

We rely on a Gaussian equivalence property. In the limit of large degree  $d = \Theta(N)$ ,  $\tilde{A}$  can be approximated by the following spiked matrix  $A^g \in \mathbb{R}^{N \times N}$ , without changing the expected losses and accuracies of the model [15, 8, 21]

$$A^g = \frac{\lambda}{\sqrt{N}}yy^T + \Xi, \quad (15)$$

where  $\Xi$  are random fluctuations, whose components  $\Xi_{ij}$  are independent standard Gaussians. This equivalence should also hold for the more general case  $d = \omega(1)$ ; more precisions are given in appendix ??.

The computation is detailed in appendix A. The result is a system of self-consistent equations called the fixed-point equations. It involves twelve scalar order parameters on  $w$  and  $\sigma$ : the magnetizations  $m_w$ ,  $\hat{m}_w$ ,  $m_\sigma$  and  $\hat{m}_\sigma$ , the self-overlaps  $Q_w$ ,  $\hat{Q}_w$ ,  $Q_\sigma$  and  $\hat{Q}_\sigma$ , and the variances  $V_w$ ,  $\hat{V}_w$ ,  $V_\sigma$  and  $\hat{V}_\sigma$ . In the following,  $y$ ,  $u$ ,  $z$ ,  $\xi$ ,  $\zeta$  and  $\chi$  are reals.

### 3.1 CSBM

We define the potentials

$$\psi_w(w) = -r\gamma(w) - \frac{1}{2}\hat{V}_w w^2 + \left( \xi\sqrt{\hat{Q}_w} + u\hat{m}_w \right) w \quad (16)$$

$$\begin{aligned} \psi_{\text{out}}(h, \sigma; \bar{t}) = & -\bar{t}l(yh) - \frac{1}{2}\hat{V}_\sigma \sigma^2 + \left( \xi\sqrt{\hat{Q}_\sigma} + y\hat{m}_\sigma \right) \sigma \\ & + \log \mathcal{N}(h|c\sigma + \lambda ym_\sigma + \sqrt{Q_\sigma}\zeta, V_\sigma) + \log \mathcal{N}(\sigma|\sqrt{\mu}ym_w + \sqrt{Q_w}\chi, V_w) \end{aligned} \quad (17)$$

where  $\mathcal{N}(\cdot|m, V)$  is a scalar Gaussian density of mean  $m$  and variance  $V$ . The parameter  $\bar{t} \in \{0, 1\}$  controls if a given node is revealed  $\bar{t} = 1$  or not  $\bar{t} = 0$ . We introduce the extremizers of these potentials:

$$w^* = \underset{w}{\operatorname{argmax}} \psi_w(w) \quad (18)$$

$$(h^*, \sigma^*) = \underset{h, \sigma}{\operatorname{argmax}} \psi_{\text{out}}(h, \sigma; \bar{t} = 1) \quad (19)$$

$$(h'^*, \sigma'^*) = \underset{h, \sigma}{\operatorname{argmax}} \psi_{\text{out}}(h, \sigma; \bar{t} = 0). \quad (20)$$

For compactness we introduce the operator  $\mathcal{P}$  that, for a polynomial  $Q$  in  $h$  and  $\sigma$ , acts according to

$$\mathcal{P}(Q(h, \sigma)) = \rho Q(h^*, \sigma^*) + (1 - \rho)Q(h'^*, \sigma'^*). \quad (21)$$

For instance  $\mathcal{P}(\sigma^2) = \rho(\sigma^*)^2 + (1 - \rho)(\sigma'^*)^2$ . The fixed-point equations are

$$m_w = \frac{1}{\alpha} \mathbb{E}_{u, \xi} uw^* \quad m_\sigma = \mathbb{E}_{y, \xi, \zeta, \chi} y\mathcal{P}(\sigma) \quad (22)$$

$$Q_w = \frac{1}{\alpha} \mathbb{E}_{u, \xi} (w^*)^2 \quad Q_\sigma = \mathbb{E}_{y, \xi, \zeta, \chi} \mathcal{P}(\sigma^2) \quad (23)$$

$$V_w = \frac{1}{\alpha} \frac{1}{\sqrt{\hat{Q}_w}} \mathbb{E}_{u, \xi} \xi w^* \quad V_\sigma = \frac{1}{\sqrt{\hat{Q}_\sigma}} \mathbb{E}_{y, \xi, \zeta, \chi} \xi \mathcal{P}(\sigma) \quad (24)$$

$$\hat{m}_w = \frac{\sqrt{\mu}}{V_w} \mathbb{E}_{y,\xi,\zeta,\chi} y \mathcal{P}(\sigma - \sqrt{\mu} y m_w) \quad (25)$$

$$\hat{Q}_w = \frac{1}{V_w^2} \mathbb{E}_{y,\xi,\zeta,\chi} \mathcal{P}((\sigma - \sqrt{\mu} y m_w - \sqrt{Q_w} \chi)^2) \quad (26)$$

$$\hat{V}_w = \frac{1}{V_w} \left( 1 - \frac{1}{\sqrt{Q_w}} \mathbb{E}_{y,\xi,\zeta,\chi} \chi \mathcal{P}(\sigma) \right) \quad (27)$$

$$\hat{m}_\sigma = \frac{\lambda}{V_\sigma} \mathbb{E}_{y,\xi,\zeta,\chi} y \mathcal{P}(h - c\sigma - \lambda y m_\sigma) \quad (28)$$

$$\hat{Q}_\sigma = \frac{1}{V_\sigma^2} \mathbb{E}_{y,\xi,\zeta,\chi} \mathcal{P}((h - c\sigma - \lambda y m_\sigma - \sqrt{Q_\sigma} \zeta)^2) \quad (29)$$

$$\hat{V}_\sigma = \frac{1}{V_\sigma} \left( 1 - \frac{1}{\sqrt{Q_\sigma}} \mathbb{E}_{y,\xi,\zeta,\chi} \zeta \mathcal{P}(h - c\sigma) \right). \quad (30)$$

In the expectations  $y$  is taken Rademacher and  $u, \xi, \zeta$  and  $\chi$  are standard Gaussians. A fixed-point of these equations (22)-(30) can be computed numerically by repeated updates of the order parameters until convergence. Once a fixed-point is found the expected errors and accuracies are

$$E_{\text{train}} = \mathbb{E}_{y,\xi,\zeta,\chi} l(yh^*) \quad \text{Acc}_{\text{train}} = \mathbb{E}_{y,\xi,\zeta,\chi} \delta_{y=\text{sign}(h^*)} \quad (31)$$

$$E_{\text{test}} = \mathbb{E}_{y,\xi,\zeta,\chi} l(yh'^*) \quad \text{Acc}_{\text{test}} = \mathbb{E}_{y,\xi,\zeta,\chi} \delta_{y=\text{sign}(h'^*)}. \quad (32)$$

### 3.2 GLM–SBM

The potentials are the same as for the CSBM (16)-(17); they are taken at  $\mu = 0$ . The extremizers  $w^*, (h^*, \sigma^*)$  and  $(h'^*, \sigma'^*)$  are defined as in (18)-(20). For compactness we introduce

$$\eta_w = \alpha \frac{m_w^2}{Q_w} \quad \text{and} \quad g(\chi) = \frac{e^{-\frac{\eta_w}{2(1-\eta_w)} \chi^2}}{\sqrt{2\pi\alpha^{-1}(1-\eta_w)}}. \quad (33)$$

The fixed-point equations are

$$m_w = \frac{1}{\alpha} \mathbb{E}_{u,\xi} u w^* \quad m_\sigma = \mathbb{E}_{\xi,\zeta,\chi} \mathbb{E}_y y \mathcal{P}(\sigma) \quad (34)$$

$$Q_w = \frac{1}{\alpha} \mathbb{E}_{u,\xi} (w^*)^2 \quad Q_\sigma = \mathbb{E}_{\xi,\zeta,\chi} \mathbb{E}_y \mathcal{P}(\sigma^2) \quad (35)$$

$$V_w = \frac{1}{\alpha} \frac{1}{\sqrt{\hat{Q}_w}} \mathbb{E}_{u,\xi} \xi w^* \quad V_\sigma = \frac{1}{\sqrt{\hat{Q}_\sigma}} \mathbb{E}_{\xi,\zeta,\chi} \mathbb{E}_y \xi \mathcal{P}(\sigma) \quad (36)$$

$$\hat{m}_w = \frac{1}{V_w} \mathbb{E}_{\xi,\zeta,\chi} \sum_{y=\pm 1} y g(\chi) \mathcal{P}(\sigma) \quad (37)$$

$$\hat{Q}_w = \frac{1}{V_w^2} \mathbb{E}_{\xi,\zeta,\chi} \mathbb{E}_y \mathcal{P}((\sigma - \sqrt{Q_w} \chi)^2) \quad (38)$$

$$\hat{V}_w = \frac{1}{V_w} \left( 1 - \frac{1}{\sqrt{Q_w}} \mathbb{E}_{\xi,\zeta,\chi} \left( \mathbb{E}_y \chi \mathcal{P}(\sigma) - \sum_{y=\pm 1} \frac{y m_w}{\sqrt{Q_w}} g(\chi) \mathcal{P}(\sigma) \right) \right) \quad (39)$$

$$\hat{m}_\sigma = \frac{\lambda}{V_\sigma} \mathbb{E}_{\xi,\zeta,\chi} \mathbb{E}_y y \mathcal{P}(h - c\sigma - \lambda y m_\sigma) \quad (40)$$

$$\hat{Q}_\sigma = \frac{1}{V_\sigma^2} \mathbb{E}_{\xi,\zeta,\chi} \mathbb{E}_y \mathcal{P}((h - c\sigma - \lambda y m_\sigma - \sqrt{Q_\sigma} \zeta)^2) \quad (41)$$

$$\hat{V}_\sigma = \frac{1}{V_\sigma} \left( 1 - \frac{1}{\sqrt{Q_\sigma}} \mathbb{E}_{\xi,\zeta,\chi} \mathbb{E}_y \zeta \mathcal{P}(h - c\sigma) \right). \quad (42)$$

In the expectations,  $y = \pm 1$  with probability

$$P(y) = \frac{1}{2} \left( 1 + y \operatorname{erf} \left( \frac{m_w \chi}{\sqrt{2\alpha^{-1} Q_w (1 - \eta_w)}} \right) \right) \quad (43)$$

and  $u$ ,  $\xi$ ,  $\zeta$  and  $\chi$  are standard Gaussians. Once a fixed-point of these equations (34)-(42) is found the expected errors and accuracies are given by

$$E_{\text{train}} = \mathbb{E}_{\xi, \zeta, \chi} \mathbb{E}_y l(yh^*) \quad (44)$$

$$E_{\text{test}} = \mathbb{E}_{\xi, \zeta, \chi} \mathbb{E}_y l(yh'^*) \quad (45)$$

## 4 Results and rates of the generalization error

### 4.1 Optimal regularization, self-loop strength and loss

We search for the parameters of the GCN that optimize the test accuracy: we can tune the self-loop intensity  $c$ , the regularization strength  $r$  and the type of the loss  $l$ . We consider only  $l_2$ -regularization since we are in a simple setting not involving sparsity or outliers where  $l_1$ -regularization would have been beneficial. We consider both low and high snr, on both the CSBM and the GLM–SBM. We keep the signals of the graph and the features balanced. We take  $\rho = 0.1$  to mimic the common case where relatively few train labels are available.

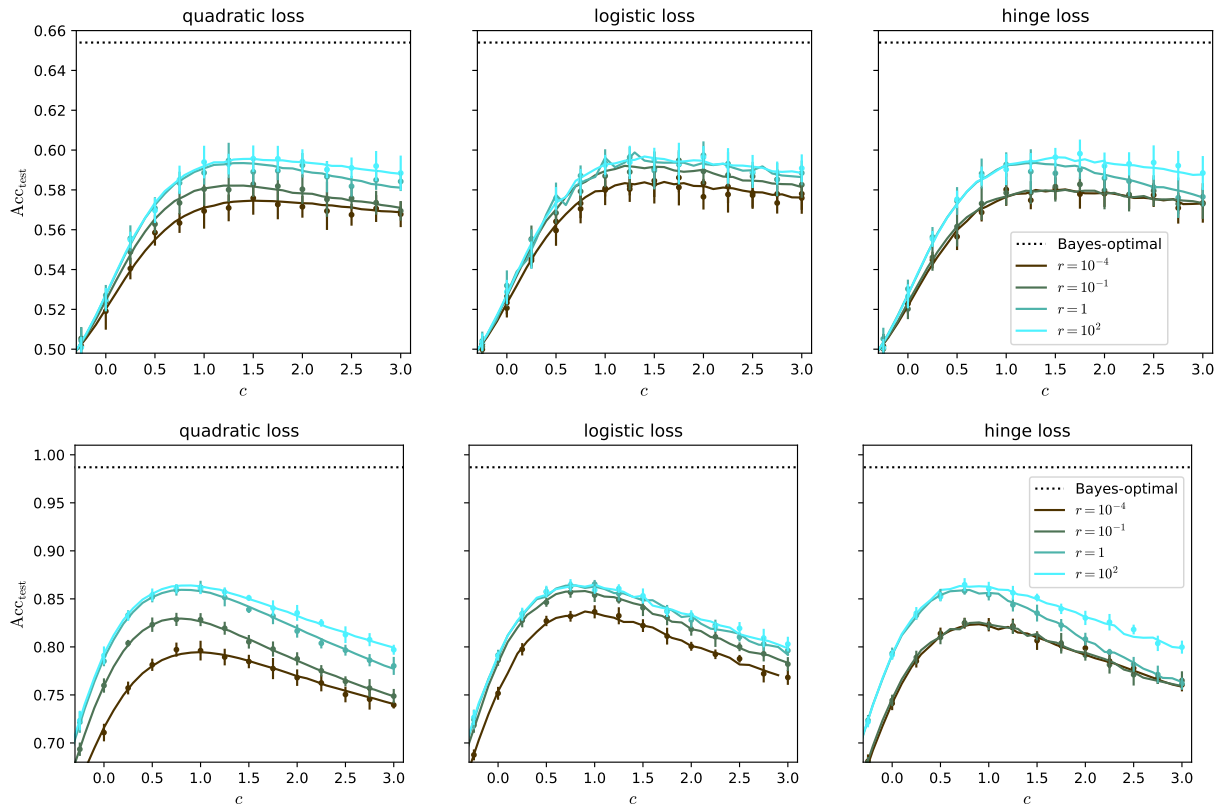


Figure 1: Search for the optimal parameters of the GCN on CSBM.  $\alpha = 4$ ,  $\rho = 0.1$ . Top: low snr,  $\lambda = 0.5$ ,  $\mu = 1$ . Bottom: high snr,  $\lambda = 1.5$ ,  $\mu = 3$ . Full lines: test accuracies predicted by (22)-(32); dots: numerical simulation of the GCN for  $N = 10^4$  and  $d = N/2$ , averaged over ten experiments; dotted line: Bayes-optimal test accuracy.

The predicted test accuracies are shown in Figs. 1 and 2 for different values of the parameters of the GCN. Our theoretical predictions are compared to simulations of the GCN for  $N = 10^4$ . As expected, the predicted test accuracy, train accuracy and errors are within the statistical errors; see also Fig. 5 in appendix D.

We observe that for all self-loop strengths  $c$  the test accuracy increases with the regularization  $r$  and reaches an optimal value at  $r \rightarrow \infty$ . The optimal  $c$  is close to 1. This is consistent with [21] that shows  $c$

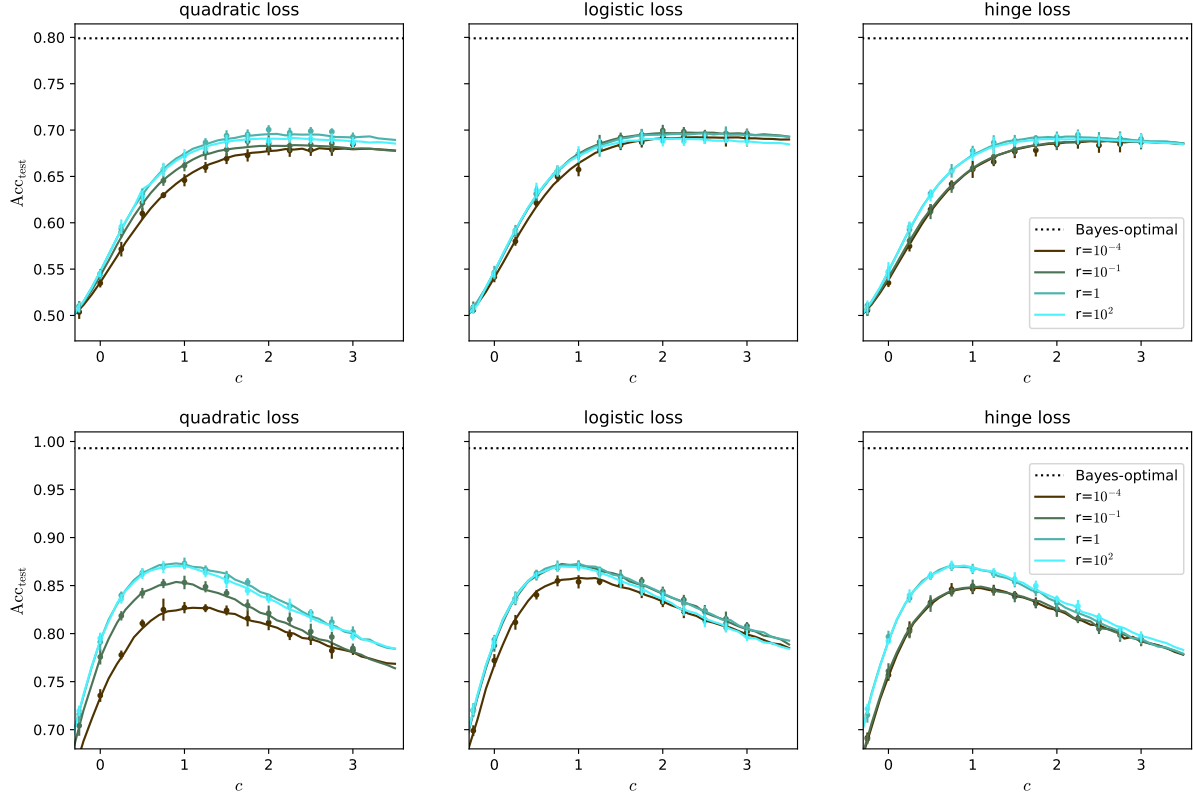


Figure 2: Search for the optimal parameters of the GCN on GLM–SBM.  $\alpha = 4$ ,  $\rho = 0.1$ . Top: low snr,  $\lambda = 0.5$ . Bottom: high snr,  $\lambda = 1.5$ . Full lines: test accuracies predicted by (34)–(45); dots: numerical simulation of the GCN for  $N = 10^4$  and  $d = N/2$ , averaged over ten experiments; dotted line: Bayes-optimal test accuracy.

positive improves inference on homophilic graphs. At low regularization  $r$  we checked that interpolation peaks appear for the different losses while varying  $\alpha$  or  $\rho$ ; see Fig. 5 in appendix D. Increasing  $r$  smooths the peaks out, as [21] shows for the quadratic loss; and as it is well known for the feedforward networks, see e.g. [18].

A surprising result seen in Figs. 1 and 2 is that the optimal accuracy does not depend significantly on the loss; in particular, we do not see any significant difference between the three considered losses at large regularization  $r$ . This is striking because it is rather generically anticipated that for classification the quadratic loss is less suitable than the logistic or hinge losses. Indeed, in the feed-forward setting, [1] showed that the optimally regularized logistic regression improves significantly on the ridge regression. We do not observe such improvement in the present single-layer GCN setting where the convolution  $P(A)X$  on the graph mixes the features.

Another remarkable point seen in Figs. 1 and 2 is that the performances of the GCN are far from the Bayes-optimal performances (dotted lines in the two figures) in all cases. This is a major difference with the feedforward case [1, 18], which shows that well-regularized regression performs very closely to the Bayes-optimal accuracy. One could argue that this can be expected since the GCN performs only one step of convolution; estimators  $P(A)Xw$  with a higher-order polynomial  $P$  could be better. Yet such a gap exists even for more elaborated GNNs on CSBM [10] and GLM–SBM [9].

In the next part we show that the one-layer GCN, while being consistent, does not reach the Bayes-optimal learning rate at large graph snr  $\lambda$ .

## 4.2 Learning rates in the high snr regime

The systems of equations (22)-(30) and (34)-(42) can be solved analytically for ridge regression, where the regularization is  $\gamma(x) = x^2/2$  and the loss is  $l(x) = (1 - x^2)/2$ . The corresponding fixed-point equations are given in appendix A.3, for  $c = 0$  to have simple expressions. As we will see, in the high snr regime this choice has negligible effect on the rates we are interested in. The ridge-less limit  $r = 0$  and  $\alpha\rho > 1$  has been studied by [21] for the CSBM. We checked that our explicit expressions for the errors and the accuracies match theirs.

In the following, we consider the large regularization limit  $r \rightarrow \infty$ . As we saw in the previous section this limit is of particular relevance since it corresponds to the optimal test performance of the GCN. Also, as we discussed, while the following results are derived for the quadratic loss, they are very close for the other considered losses.

**Bayes-optimal:** We will compare to the optimal learning rates that are explicit in the limit of large graph snr. Taking  $\lambda \rightarrow \infty$  in the equations in appendix B, for both the CSBM and the GLM-SBM, the Bayes-optimal test accuracy is

$$\text{Acc}_{\text{test}}^{\text{BO}} = \frac{1}{2} (1 + \text{erf}(\lambda\sqrt{\tau_{\text{BO}}})) , \quad \tau_{\text{BO}} = 1 . \quad (46)$$

The convergence to perfect recovery is exponentially fast in  $\lambda^2$ : we have  $\log(1 - \text{Acc}_{\text{test}}^{\text{BO}}) \sim -\lambda^2\tau_{\text{BO}}$ , with  $\tau_{\text{BO}} = 1$  the Bayes-optimal rate. We remind that  $\text{erfc} = 1 - \text{erf}$  and  $\log \text{erfc}(x) \underset{x \rightarrow \infty}{\sim} -x^2$ .

**CSBM:** We now consider the CSBM learned with a GCN with  $c = 0$  and ridge regularization  $r \rightarrow \infty$ , first at an arbitrary snr  $\lambda$ . An explicit formula for the test accuracy is

$$\text{Acc}_{\text{test}} = \frac{1}{2} (1 + \text{erf}(\lambda\sqrt{\tau_{\text{CSBM}}})) \quad (47)$$

$$\sqrt{\tau_{\text{CSBM}}} = \frac{\lambda\rho(1 + \mu)}{\sqrt{2}\sqrt{\rho(1 + \alpha) + \lambda^2\rho^2(1 + \mu)(1 + \alpha + \mu)}} , \quad (48)$$

where we defined  $\tau_{\text{CSBM}}$  the learning rate or convergence rate of the GCN on the CSBM.

For large graph snr  $\lambda$  the GCN is consistent, it reaches perfect recovery. The difference to perfect recovery is

$$\log(1 - \text{Acc}_{\text{test}}) \underset{\lambda \rightarrow \infty}{\sim} -\lambda^2\tau_{\text{CSBM}} . \quad (49)$$

The greater  $\tau_{\text{CSBM}}$  the fastest the convergence is.

$\tau_{\text{CSBM}}$  can be expressed in a simpler form at in the limit of large snr  $\lambda$ :

$$\tau_{\text{CSBM}} \xrightarrow{\lambda \rightarrow \infty} \tau_{\text{CSBM}}^\infty = \frac{1 + \mu}{2(1 + \alpha + \mu)} . \quad (50)$$

This expression highlights the importance of the features: even at large graph snr  $\lambda$  the GCN relies on the snr  $\mu$  of the features. Indeed  $\tau_{\text{CSBM}}^\infty$  is increasing with  $\mu$ , from  $1/2(1 + \alpha)$  at  $\mu = 0$  to  $1/2$  at large  $\mu$ . As suggested by the expression of the snr of the CSBM (3), increasing  $\alpha$  lowers the performance, since  $\tau_{\text{CSBM}}^\infty$  goes to zero for large  $\alpha$ . The respective snrs  $\mu$  and  $\alpha$  do not contribute to  $\tau_{\text{CSBM}}^\infty$  in the same manner as in (3) where only the ratio  $\mu^2/\alpha$  matters. This is a sign that the GCN does not handle the features in an optimal way.

The GCN also seems not to handle the graph optimally. Indeed the Bayes-optimal rate  $\tau_{\text{BO}} = 1$  does not depend on the feature snr  $\mu$ : hence the graph alone is sufficient to reach the Bayes-optimal rate. We also notice that none of these rates depend on the training ratio  $\rho$ .

We can also use these expressions to predict the performance of the GCN on the canonical SBM without features. More precisely,  $\mu = 0$  corresponds to a SBM populated with random Gaussian features. The rate reached by the GCN is better when  $\alpha = \frac{N}{M} \rightarrow 0$  i.e. when we take the dimension  $M$  as large as possible.

Finally, let us justify why we discussed the rates for  $c = 0$ . This is because at  $\lambda \rightarrow \infty$ , the learning rates  $\tau_{\text{CSBM}}$  and  $\tau_{\text{CSBM}}^\infty$ , while being derived for  $c = 0$ , describe the optimal performance of the GCN for optimal  $c$  as well. This is shown in Fig. 3,  $\tau_{\text{CSBM}}^\infty$  fits perfectly the accuracy of the GCN whose  $c$  is optimized for

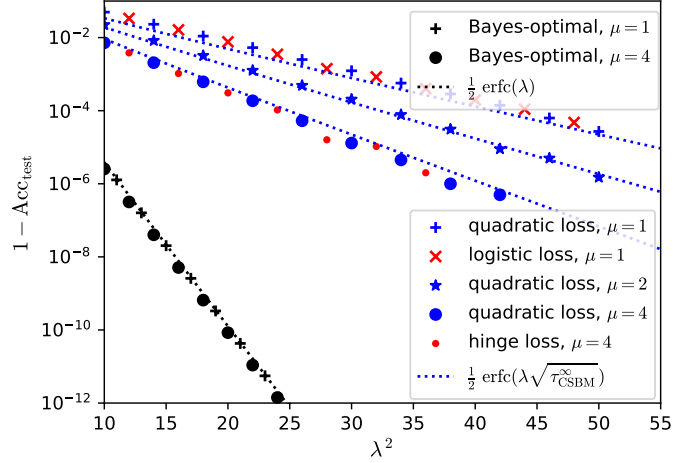


Figure 3: Asymptotic misclassification error  $1 - \text{Acc}_{\text{test}}$  on the CSBM.  $\alpha = 4$ ,  $\rho = 0.1$ . Dots: test accuracies predicted by (22)-(32), for  $r = 10^3$  and optimal  $c$  (the optimal  $c$  is always between 0 and 1). Dotted lines: approximation given by (50). The Bayes-optimal values are obtained from the equations given in appendix B.

the three different losses. Optimizing on  $c$  leads only to a sub-leading improvement in the limit  $\lambda \rightarrow \infty$ . As anticipated, Fig. 3 also shows that the three different losses give equal performances and the same rates.

In conclusion, Fig. 3 further illustrates that the GCN does not reach the Bayes-optimal rate. For all considered settings  $\tau_{\text{CSBM}}^\infty$  is bounded by  $1/2$  while  $\tau_{\text{BO}} = 1$ . Moreover  $\tau_{\text{CSBM}}^\infty$  reaches its upper bound  $1/2$  only for the feature snr  $\mu$  diverging or  $\alpha$  going to zero, which confirms that the considered GCN has a poor performance.

**GLM–SBM** We consider now the GLM–SBM in the same setting  $c = 0$  and  $r \rightarrow \infty$  for ridge regression, first at any  $\lambda$ . We obtain an explicit formula for the test accuracy

$$\text{Acc}_{\text{test}} = \frac{1}{2} (1 + \text{erf}(\lambda \sqrt{\tau_{\text{GLM-SBM}}})) \quad (51)$$

$$\sqrt{\tau_{\text{GLM-SBM}}} = \frac{\lambda \rho (1 + 2\alpha/\pi)}{\sqrt{2} \sqrt{\rho(1 + \alpha) + \lambda^2 \rho^2 a(\alpha)}} \quad (52)$$

$$a(\alpha) = (1 + 2\alpha/\pi)(1 + \alpha + 2\alpha/\pi) - 4\alpha^2/\pi^2, \quad (53)$$

where we defined in the same manner  $\tau_{\text{GLM-SBM}}$  the learning rate of the GCN on the GLM–SBM. The GCN is consistent; it reaches perfect recovery for large  $\lambda$  on the GLM–SBM and its convergence rate is  $\tau_{\text{GLM-SBM}}$ .

At large graph snr  $\lambda$  its rate can be expressed more simply as

$$\tau_{\text{GLM-SBM}} \xrightarrow{\lambda \rightarrow \infty} \tau_{\text{GLM-SBM}}^\infty = \frac{1 + 2\alpha/\pi}{2 \left( 1 + \alpha + \frac{2\alpha/\pi}{1 + 2\alpha/\pi} \right)}. \quad (54)$$

We see a strong similitude between  $\tau_{\text{GLM-SBM}}^\infty$  and  $\tau_{\text{CSBM}}^\infty$  or between  $\tau_{\text{GLM-SBM}}$  and  $\tau_{\text{CSBM}}$ . It is as if the feature snr  $\mu$  of the CSBM were equivalent to an effective feature snr  $2\alpha/\pi$  for the GLM–SBM. This is consistent with the expressions of the feature snrs of the two models (3) and (5), that are  $\mu^2/\alpha$  and  $4\alpha/\pi^2$ .

$\tau_{\text{GLM-SBM}}^\infty$  converges to a finite value for large  $\alpha$ , contrary to  $\tau_{\text{CSBM}}^\infty$  that goes to zero. This could be expected since the snr of the GLM–SBM (5) is increasing with  $\alpha$ . A less intuitive result is that  $\tau_{\text{GLM-SBM}}^\infty$  reaches its maximum for  $\alpha$  going to zero, as for  $\tau_{\text{CSBM}}^\infty$ . It seems that for the GCN there is a trade-off between the feature snr from the GLM (increasing with  $\alpha$ ) and the the resulting feature snr of the convoluted features  $P(A)X$  (decreasing with  $\alpha$ ).

As for the CSBM, the learning rate  $\tau_{\text{CSBM}}$  well describes the optimal performance of the GCN even when  $c$  is tuned. We can see in Fig. 4 that optimizing on  $c$  only leads to a sub-leading improvement: the predicted values follow the slopes given by  $\tau_{\text{CSBM}}$  up to a constant shift.

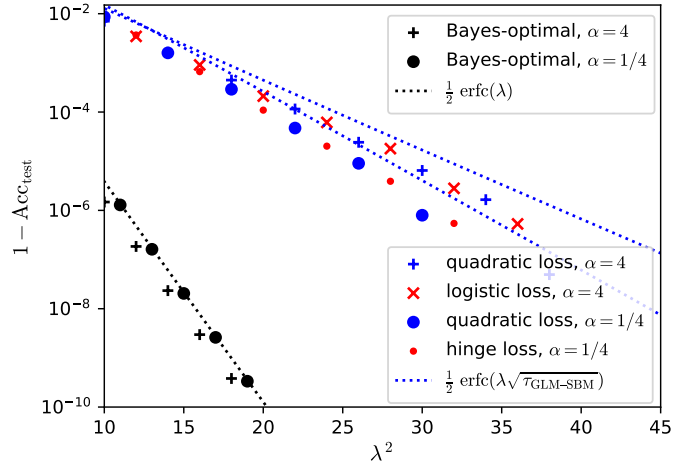


Figure 4: Asymptotic misclassification error  $1 - \text{Acc}_{\text{test}}$  on the GLM-SBM.  $\rho = 0.1$ . Dots: test accuracies predicted by (34)-(45), for  $r = 10^3$  and optimal  $c$  (the optimal  $c$  is always between 0 and 1). Dotted line: predicted rate  $\tau_{\text{GLM-SBM}}$  eq. (52) for quadratic loss,  $c = 0$  and large regularization  $r$ . We did not use the approximation  $\tau_{\text{GLM-SBM}}^\infty$  because for  $\alpha = 1/4$  we were not able to reach  $\lambda$  large enough. The Bayes-optimal values are obtained from the equations given in appendix B.

Again the GCN is not able to equalize the Bayes-optimal rate. For all considered settings  $\tau_{\text{CSBM}}^\infty$  is upper-bounded by  $1/2$  and reaches the bound only for the aspect ratio  $\alpha$  going to zero.

## 5 Conclusion

We theoretically predicted the generalization performances of a one-layer GCN on two models of attributed graphs. We showed that the optimal test accuracy is achieved for a finite value of the self-loop intensity at large regularization and does not depend visibly on the training loss. This stands both when the features and the labels are generated by a Gaussian mixture and when they are generated by a GLM. We derived the optimal learning rates of the GCN and showed they can be interpreted in terms of feature signal-to-noise ratios. The GCN is consistent at large graph snr but does not reach the Bayes-optimal rate.

A future direction of work could be to analyze more complex GNNs such as a GCN with higher-order graph convolution  $P(A)$  or an attention-based GNN and to see if they can reach the Bayes-optimality. Another direction could be given by the work [20] that proposes a model for genes where the components of the features are correlated according to a graph. One could study the role of a graph-induced regularization.

## Acknowledgements

We acknowledge discussions with Cheng Shi. This work is supported by the Swiss National Science Foundation under grant SNFS SMArtNet (grant number 212049).

## References

- [1] Benjamin Aubin, Florent Krzakala, Yue M. Lu, and Lenka Zdeborová. Generalization error in high-dimensional perceptrons: Approaching Bayes error with convex optimization. In *Advances in Neural Information Processing Systems*, 2020. arxiv:2006.06560.
- [2] Benjamin Aubin, Bruno Loureiro, Antoine Maillard, Florent Krzakala, and Lenka Zdeborová. The spiked matrix model with generative priors. In *Advances in Neural Information Processing Systems*, 2019. arxiv:1905.12385.

- [3] Aseem Baranwal, Kimon Fountoulakis, and Aukosh Jagannath. Graph convolution for semi-supervised classification: Improved linear separability and out-of-distribution generalization. In *Proceedings of the 38th International Conference on Machine Learning*, 2021. arxiv:2102.06966.
- [4] Aseem Baranwal, Kimon Fountoulakis, and Aukosh Jagannath. Optimality of message-passing architectures for sparse graphs. In *37th Conference on Neural Information Processing Systems*, 2023. arxiv:2305.10391.
- [5] Jean Barbier, Florent Krzakala, Nicolas Macris, Léo Miolane, and Lenka Zdeborová. Optimal errors and phase transitions in high-dimensional generalized linear models. *Proceedings of the National Academy of Sciences*, 116(12):5451–5460, 2019.
- [6] Eli Chien, Jianhao Peng, Pan Li, and Olgica Milenkovic. Adaptative universal generalized pagerank graph neural network. In *International Conference on Learning Representations*, 2021. arxiv:2006.07988.
- [7] Weilin Cong, Morteza Ramezani, and Mehrdad Mahdavi. On provable benefits of depth in training graph convolutional networks. 2021. arxiv:2110.15174.
- [8] Yash Deshpande, Subhabrata Sen, Andrea Montanari, and Elchanan Mossel. Contextual stochastic block models. In S. Bengio, H. Wallach, H. Larochelle, K. Grauman, N. Cesa-Bianchi, and R. Garnett, editors, *Advances in Neural Information Processing Systems*, volume 31, 2018. arxiv:1807.09596.
- [9] O Duranthon and L Zdeborová. Neural-prior stochastic block model. *MLST*, 2023. arxiv:2303.09995.
- [10] O Duranthon and L Zdeborová. Optimal inference in contextual stochastic block models. 2023. arxiv:2306.07948.
- [11] Pascal Mattia Esser, Leena Chennuru Vankadara, and Debarghya Ghoshdastidar. Learning theory can (sometimes) explain generalisation in graph neural networks. In *35th Conference on Neural Information Processing Systems*, 2021. arXiv:2112.03968.
- [12] Guoji Fu, Peilin Zhao, and Yatao Bian. p-Laplacian based graph neural networks. In *Proceedings of the 39th International Conference on Machine Learning*, 2022. arxiv:2111.07337.
- [13] Haotian Ju, Dongyue Li, Aneesh Sharma, and Hongyang R. Zhang. Generalization in graph neural networks: Improved PAC-Bayesian bounds on graph diffusion. In *AISTATS*, 2023. arXiv:2302.04451.
- [14] Runlin Lei, Zhen Wang, Yaliang Li, Bolin Ding, and Zhewei Wei. EvenNet: Ignoring odd-hop neighbors improves robustness of graph neural networks. In *36th Conference on Neural Information Processing Systems*, 2022. arxiv:2205.13892.
- [15] Thibault Lesieur, Florent Krzakala, and Lenka Zdeborová. Constrained low-rank matrix estimation: Phase transitions, approximate message passing and applications. *Journal of Statistical Mechanics: Theory and Experiment*, 2017(7):073403, 2017. arxiv:1701.00858.
- [16] Chen Lu and Subhabrata Sen. Contextual stochastic block model: Sharp thresholds and contiguity. 2020. arXiv:2011.09841.
- [17] Song Mei and Andrea Montanari. The generalization error of random features regression: Precise asymptotics and the double descent curve. *Communications on Pure and Applied Mathematics*, 75(4):667–766, 2022.
- [18] Francesca Mignacco, Florent Krzakala, Yue M. Lu, and Lenka Zdeborová. The role of regularization in classification of high-dimensional noisy Gaussian mixture. In *International conference on learning representations*, 2020. arxiv:2002.11544.
- [19] Andrea Montanari, Feng Ruan, Youngtak Sohn, and Jun Yan. The generalization error of max-margin linear classifiers: High-dimensional asymptotics in the overparametrized regime. *arXiv preprint arXiv:1911.01544*, 2019.

- [20] Sagnik Nandy and Subhabrata Sen. Bayes optimal learning in high-dimensional linear regression with network side information. 2023. arxiv:2306.05679.
- [21] Cheng Shi, Liming Pan, Hong Hu, and Ivan Dokmanić. Statistical mechanics of generalization in graph convolution networks. 2022. arXiv:2212.13069.
- [22] Huayi Tang and Yong Liu. Towards understanding the generalization of graph neural networks. 2023. arXiv:2305.08048.
- [23] Bowei Yan and Purnamrita Sarkar. Covariate regularized community detection in sparse graphs. *Journal of the American Statistical Association*, 116(534):734–745, 2021. arxiv:1607.02675.
- [24] Chiyuan Zhang, Samy Bengio, Moritz Hardt, Benjamin Recht, and Oriol Vinyals. Understanding deep learning (still) requires rethinking generalization. *Communications of the ACM*, 64(3):107–115, 2021.

## A Replica computation

In this appendix, we derive the equations given in section 3 of the main text.

### A.1 CSBM

We first derive the results for the CSBM, generalizing the results of [21] to arbitrary convex loss and regularization. As stated in eq. (14), we introduce  $n$  replica:

$$\log Z = \frac{\partial}{\partial n} Z^n(n=0) \quad (55)$$

$$-\beta N f = \frac{\partial}{\partial n}(n=0) \mathbb{E}_{u, \Xi, W, y} \underbrace{\int \prod_a^n \prod_{\nu} dw_{\nu}^a P_W(w_{\nu}^a) e^{\sum_a^n -\beta t \sum_{i \in R} l(y_i h(w^a)_i) - \beta t' \sum_{i \in R'} l(y_i h(w^a)_i)}}_{*} \quad (56)$$

where  $P_W(w) = \exp(-\beta r \gamma(w))$  is the prior on the weights induced by the regularization. We introduce several ancillary variables via  $\delta$ -Dirac functions to decouple the random variables. We set  $h = \frac{1}{\sqrt{N}}(A + c\sqrt{N}I_N)\sigma$  and  $\sigma = \frac{1}{\sqrt{N}}Xw$ . Then we take the expectation on the Gaussian noise:

$$* \propto \mathbb{E}_{u, \Xi, W, y} \int \prod_{a, \nu} dw_{\nu}^a P_W(w_{\nu}^a) \prod_{a, i} dh_i^a dq_i^a e^{-\beta t \sum_{a, i \in R} l(y_i h_i^a) - \beta t' \sum_{a, i \in R'} l(y_i h_i^a) + \sum_{a, i} i q_i^a (h_i^a - h(w^a)_i)} \quad (57)$$

$$= \mathbb{E}_{u, \Xi, W, y} \int \prod_{a, \nu} dw_{\nu}^a P_W(w_{\nu}^a) \prod_{a, i} dh_i^a dq_i^a d\sigma_i^a d\hat{q}_i^a e^{-\beta t \sum_{a, i \in R} l(y_i h_i^a) - \beta t' \sum_{a, i \in R'} l(y_i h_i^a)} \\ e^{\sum_{a, i} i q_i^a (h_i^a - \frac{1}{\sqrt{N}} \sum_j (c\sqrt{N} \delta_{i, j} + \frac{\lambda}{\sqrt{N}} y_i y_j + \Xi_{ij}) \sigma_j^a) + \sum_{a, i} i \hat{q}_i^a (\sigma_i^a - \frac{1}{\sqrt{N}} \sum_{\nu} (\sqrt{\frac{\mu}{N}} y_j u_{\nu} + W_{j\nu}) w_{\nu}^a)} \quad (58)$$

$$= \mathbb{E}_{u, y} \int \prod_{a, \nu} dw_{\nu}^a P_W(w_{\nu}^a) \prod_{a, i} dh_i^a dq_i^a d\sigma_i^a d\hat{q}_i^a e^{-\beta t \sum_{a, i \in R} l(y_i h_i^a) - \beta t' \sum_{a, i \in R'} l(y_i h_i^a) + i \sum_{a, i} (q_i^a h_i^a + \hat{q}_i^a \sigma_i^a)} \\ e^{-i \sum_{a, i} (cq_i^a \sigma_i^a + \frac{\lambda}{N} y_i q_i^a \sum_j y_j \sigma_j^a) - \frac{1}{2N} \sum_{i, j, a, b} q_i^a q_j^b \sigma_i^a \sigma_j^b - i \sum_{a, i} \frac{\sqrt{\mu}}{N} y_i \hat{q}_i^a \sum_{\nu} u_{\nu} w_{\nu}^a - \frac{1}{2N} \sum_{i, \nu, a, b} \hat{q}_i^a \hat{q}_i^b w_{\nu}^a w_{\nu}^b}. \quad (59)$$

We integrate over the  $qs$  and  $\hat{qs}$ . For simplicity we pack the replica into vectors of size  $n$ .

$$* = \mathbb{E}_{u, y} \int \prod_{a, \nu} dw_{\nu}^a P_W(w_{\nu}^a) \prod_{a, i} dh_i^a dq_i^a d\sigma_i^a d\hat{q}_i^a e^{-\beta t \sum_{a, i \in R} l(y_i h_i^a) - \beta t' \sum_{a, i \in R'} l(y_i h_i^a) + i \sum_i q_i^T (h_i - c\sigma_i - \frac{\lambda}{N} y_i \sum_j y_j \sigma_j)} \\ e^{-\frac{1}{2N} \sum_i q_i^T (\sum_j \sigma_j \sigma_j^T) q_i + i \sum_i \hat{q}_i^T (\sigma_i - \frac{\sqrt{\mu}}{N} y_i \sum_{\nu} u_{\nu} w_{\nu}^T) - \frac{1}{2N} \sum_i \hat{q}_i^T (\sum_{\nu} w_{\nu} w_{\nu}^T) \hat{q}_i} \quad (60)$$

$$= \mathbb{E}_{u, y} \int \prod_{a, \nu} dw_{\nu}^a P_W(w_{\nu}^a) \prod_{a, i} dh_i^a d\sigma_i^a e^{-\beta t \sum_{a, i \in R} l(y_i h_i^a) - \beta t' \sum_{a, i \in R'} l(y_i h_i^a)} \\ \prod_i \mathcal{N} \left( h_i \left| c\sigma_i + \frac{\lambda}{N} y_i \sum_j y_j \sigma_j, \frac{1}{N} \sum_j \sigma_j \sigma_j^T \right. \right) \mathcal{N} \left( \sigma_i \left| \frac{\sqrt{\mu}}{N} y_i \sum_{\nu} u_{\nu} w_{\nu}, \frac{1}{N} \sum_{\nu} w_{\nu} w_{\nu}^T \right. \right); \quad (61)$$

where  $\mathcal{N}(x|\mu, \Sigma) = \det(2\pi\Sigma)^{-1/2}e^{-(x-\mu)^T\Sigma^{-1}(x-\mu)/2}$  is a Gaussian density. We introduce the order parameters via new  $\delta$ -Dirac functions. We can factorize the  $i$  and  $\nu$  indices.

$$* \propto \mathbb{E}_{u,y} \int \prod_{a,\nu} dw_\nu^a P_W(w_\nu^a) \prod_{a,i} dh_i^a d\sigma_i^a \prod_{a \leq b} d\hat{Q}_w^{ab} dQ_w^{ab} d\hat{Q}_\sigma^{ab} dQ_\sigma^{ab} \prod_a d\hat{m}_w^a dm_w^a d\hat{m}_\sigma^a dm_\sigma^a e^{-\beta t \sum_{a,i \in R} l(y_i h_i^a)} e^{-\beta t' \sum_{a,i \in R'} l(y_i h_i^a)} \prod_{a \leq b} e^{\hat{Q}_w^{ab} (NQ_w^{ab} - \sum_\nu w_\nu^a w_\nu^b) + \hat{Q}_\sigma^{ab} (NQ_\sigma^{ab} - \sum_i \sigma_i^a \sigma_i^b)} \prod_a e^{\hat{m}_w^a (Nm_w^a - \sum_\nu u_\nu w_\nu^a) + \hat{m}_\sigma^a (Nm_\sigma^a - \sum_i y_i \sigma_i^a)} \prod_i N(h_i | c\sigma_i + \lambda y_i m_\sigma, Q_\sigma) \mathcal{N}(\sigma_i | \sqrt{\mu} y_i m_w, Q_w) \quad (62)$$

$$= \int \prod_{a \leq b} d\hat{Q}_w^{ab} dQ_w^{ab} d\hat{Q}_\sigma^{ab} dQ_\sigma^{ab} \prod_a d\hat{m}_w^a dm_w^a d\hat{m}_\sigma^a dm_\sigma^a \prod_{a \leq b} e^{N(\hat{Q}_w^{ab} Q_w^{ab} + \hat{Q}_\sigma^{ab} Q_\sigma^{ab})} \prod_a e^{N(\hat{m}_w^a m_w^a + \hat{m}_\sigma^a m_\sigma^a)} \left[ \mathbb{E}_u \int \prod_a dw^a e^{\psi_w^{(n)}(w)} \right]^{N/\alpha} \left[ \mathbb{E}_y \int \prod_a dh^a d\sigma^a e^{\psi_{\text{out}}^{(n)}(h, \sigma; t)} \right]^{\rho N} \left[ \mathbb{E}_y \int \prod_a dh^a d\sigma^a e^{\psi_{\text{out}}^{(n)}(h, \sigma; t')} \right]^{\rho' N} \left[ \mathbb{E}_y \int \prod_a dh^a d\sigma^a e^{\psi_{\text{out}}^{(n)}(h, \sigma; 0)} \right]^{(1-\rho-\rho')N}; \quad (63)$$

where we defined

$$\psi_w^{(n)}(w) = \sum_a \log P_W(w^a) - \sum_{a \leq b} \hat{Q}_w^{ab} w^a w^b - \sum_a \hat{m}_w^a u w^a \quad (64)$$

$$\begin{aligned} \psi_{\text{out}}^{(n)}(h, \sigma; \bar{t}) &= -\beta \bar{t} \sum_a l(yh^a) - \sum_{a \leq b} \hat{Q}_\sigma^{ab} \sigma^a \sigma^b - \sum_a \hat{m}_\sigma^a y \sigma^a - \frac{1}{2} (h - c\sigma - \lambda y m_\sigma)^T Q_\sigma^{-1} (h - c\sigma - \lambda y m_\sigma) \\ &\quad - \frac{1}{2} \log \det Q_\sigma - \frac{1}{2} (\sigma - \sqrt{\mu} y m_w)^T Q_w^{-1} (\sigma - \sqrt{\mu} y m_w) - \frac{1}{2} \log \det Q_w. \end{aligned} \quad (65)$$

We use the replica-symmetric ansatz: we set  $\hat{Q}^{aa} = \frac{1}{2} \hat{R}$ ,  $\hat{Q}^{ab} = -\hat{Q}$ ,  $Q^{aa} = R$ ,  $Q^{ab} = Q$ ,  $\hat{m}^a = -\hat{m}$  and  $m^a = m$ . Since we will take the derivative wrt  $n$  and send  $n$  to zero we discard all the terms that are not proportionnal to  $n$ . We compute first that

$$Q^{-1} = \frac{1}{R - Q} I_n - \frac{Q}{(R - Q)^2} J_{n,n} + o(n) \quad (66)$$

$$\log \det Q = n \frac{Q}{R - Q} + n \log(R - Q) + o(n); \quad (67)$$

where  $J_{n,n}$  is the matrix filled with ones. We define the variances  $V = R - Q$  and  $\hat{V} = \hat{R} + \hat{Q}$ . We introduce scalar Gaussian random variables  $\xi$  and  $\chi$  to decouple the replica and factorize them. Then

$$* \propto \int d\hat{Q}_w d\hat{V}_w dQ_w dV_w d\hat{Q}_\sigma d\hat{V}_\sigma dQ_\sigma dV_\sigma d\hat{m}_w dm_w d\hat{m}_\sigma dm_\sigma e^{\frac{nN}{2} (\hat{V}_w V_w + \hat{V}_w Q_w - V_w \hat{Q}_w + \hat{V}_\sigma V_\sigma + \hat{V}_\sigma Q_\sigma - V_\sigma \hat{Q}_\sigma)} e^{-nN(\hat{m}_w m_w + \hat{m}_\sigma m_\sigma)} \left[ \mathbb{E}_{u,\xi} \left( \int dw e^{\psi_w(w)} \right)^n \right]^{N/\alpha} \left[ \mathbb{E}_{y,\xi,\zeta,\chi} \left( \int dh d\sigma e^{\psi_{\text{out}}(h, \sigma; t)} \right)^n \right]^{\rho N} \left[ \mathbb{E}_{y,\xi,\zeta,\chi} \left( \int dh d\sigma e^{\psi_{\text{out}}(h, \sigma; t')} \right)^n \right]^{\rho' N} \left[ \mathbb{E}_{y,\xi,\zeta,\chi} \left( \int dh d\sigma e^{\psi_{\text{out}}(h, \sigma; 0)} \right)^n \right]^{(1-\rho-\rho')N} \quad (68)$$

$$:= \int dm dq dv e^{N\phi^{(n)}(m, q, v)}, \quad (69)$$

with

$$\psi_w(w) = \log P_W(w) - \frac{1}{2} \hat{V}_w w^2 + \left( \xi \sqrt{\hat{Q}_w} + u \hat{m}_w \right) w \quad (70)$$

$$\begin{aligned} \psi_{\text{out}}(h, \sigma; \bar{t}) &= -\beta \bar{t} l(yh) - \frac{1}{2} \hat{V}_\sigma \sigma^2 + \left( \xi \sqrt{\hat{Q}_\sigma} + y \hat{m}_\sigma \right) \sigma \\ &+ \log \mathcal{N} \left( h | c\sigma + \lambda y m_\sigma + \sqrt{Q_\sigma} \zeta, V_\sigma \right) + \log \mathcal{N} \left( \sigma | \sqrt{\mu} y m_w + \sqrt{Q_w} \chi, V_w \right) \end{aligned} \quad (71)$$

and  $m$ ,  $q$  and  $v$  standing for all the order parameters.  $\xi$ ,  $\zeta$  and  $\chi$  are scalar standard Gaussians. We take the limit  $N \rightarrow \infty$  thanks to Laplace's method.

$$-\beta f \propto \frac{1}{N} \frac{\partial}{\partial n} (n=0) \int dm dq dv e^{N\phi^{(n)}(m,q,v)} \quad (72)$$

$$= \underset{m,q,v}{\text{extr}} \frac{\partial}{\partial n} (n=0) \phi^{(n)}(m,q,v) := \underset{m,q,v}{\text{extr}} \phi(m,q,v) ; \quad (73)$$

the free entropy is

$$\begin{aligned} \phi &= \frac{1}{2} \left( \hat{V}_w V_w + \hat{V}_w Q_w - V_w \hat{Q}_w + \hat{V}_\sigma V_\sigma + \hat{V}_\sigma Q_\sigma - V_\sigma \hat{Q}_\sigma \right) - \hat{m}_w m_w - \hat{m}_\sigma m_\sigma \\ &+ \frac{1}{\alpha} \mathbb{E}_{u,\xi} \left( \log \int dw e^{\psi_w(w)} \right) + \rho \mathbb{E}_{y,\xi,\zeta,\chi} \left( \log \int dh d\sigma e^{\psi_{\text{out}}(h,\sigma;t)} \right) \\ &+ \rho' \mathbb{E}_{y,\xi,\zeta,\chi} \left( \log \int dh d\sigma e^{\psi_{\text{out}}(h,\sigma;t')} \right) + (1 - \rho - \rho') \mathbb{E}_{y,\xi,\zeta,\chi} \left( \log \int dh d\sigma e^{\psi_{\text{out}}(h,\sigma;0)} \right) . \end{aligned} \quad (74)$$

We take the extremum of the free entropy deriving it wrt the order parameters, evaluated at  $t = 1$  and  $t' = 0$ . We obtain the following fixed-point conditions.

$$m_w = \frac{1}{\alpha} \mathbb{E}_{u,\xi} u \mathbb{E}_{P_w} w \quad m_\sigma = \mathbb{E}_{y,\xi,\zeta,\chi} y (\rho \mathbb{E}_{P_{\text{out}}} \sigma + (1 - \rho) \mathbb{E}_{P'_{\text{out}}} \sigma) \quad (75)$$

$$Q_w + V_w = \frac{1}{\alpha} \mathbb{E}_{u,\xi} (\mathbb{E}_{P_w} w)^2 \quad Q_\sigma + V_\sigma = \mathbb{E}_{y,\xi,\zeta,\chi} (\rho (\mathbb{E}_{P_{\text{out}}} \sigma)^2 + (1 - \rho) (\mathbb{E}_{P'_{\text{out}}} \sigma)^2) \quad (76)$$

$$V_w = \frac{1}{\alpha} \frac{1}{\sqrt{\hat{Q}_w}} \mathbb{E}_{u,\xi} \xi \mathbb{E}_{P_w} w \quad V_\sigma = \frac{1}{\sqrt{\hat{Q}_\sigma}} \mathbb{E}_{y,\xi,\zeta,\chi} \xi (\rho \mathbb{E}_{P_{\text{out}}} \sigma + (1 - \rho) \mathbb{E}_{P'_{\text{out}}} \sigma) \quad (77)$$

$$\hat{m}_w = \frac{\sqrt{\mu}}{V_w} \mathbb{E}_{y,\xi,\zeta,\chi} y (\rho \mathbb{E}_{P_{\text{out}}} (\sigma - \sqrt{\mu} y m_w) + (1 - \rho) \mathbb{E}_{P'_{\text{out}}} (\sigma - \sqrt{\mu} y m_w)) \quad (78)$$

$$\hat{Q}_w - \hat{V}_w = \frac{1}{V_w^2} \mathbb{E}_{y,\xi,\zeta,\chi} \left( \rho \mathbb{E}_{P_{\text{out}}} (\sigma - \sqrt{\mu} y m_w - \sqrt{Q_w} \chi)^2 + (1 - \rho) \mathbb{E}_{P'_{\text{out}}} (\sigma - \sqrt{\mu} y m_w - \sqrt{Q_w} \chi)^2 \right) - \frac{1}{V_w} \quad (79)$$

$$\hat{V}_w = \frac{1}{V_w} \left( 1 - \frac{1}{\sqrt{Q_w}} \mathbb{E}_{y,\xi,\zeta,\chi} \chi (\rho \mathbb{E}_{P_{\text{out}}} \sigma + (1 - \rho) \mathbb{E}_{P'_{\text{out}}} \sigma) \right) \quad (80)$$

$$\hat{m}_\sigma = \frac{\lambda}{V_\sigma} \mathbb{E}_{y,\xi,\zeta,\chi} y (\rho \mathbb{E}_{P_{\text{out}}} (h - c\sigma - \lambda y m_\sigma) + (1 - \rho) \mathbb{E}_{P'_{\text{out}}} (h - c\sigma - \lambda y m_\sigma)) \quad (81)$$

$$\hat{Q}_\sigma - \hat{V}_\sigma = \frac{1}{V_\sigma^2} \mathbb{E}_{y,\xi,\zeta,\chi} \left( \rho \mathbb{E}_{P_{\text{out}}} (h - c\sigma - \lambda y m_\sigma - \sqrt{Q_\sigma} \zeta)^2 + (1 - \rho) \mathbb{E}_{P'_{\text{out}}} (h - c\sigma - \lambda y m_\sigma - \sqrt{Q_\sigma} \zeta)^2 \right) - \frac{1}{V_\sigma} \quad (82)$$

$$\hat{V}_\sigma = \frac{1}{V_\sigma} \left( 1 - \frac{1}{\sqrt{Q_\sigma}} \mathbb{E}_{y,\xi,\zeta,\chi} \zeta (\rho \mathbb{E}_{P_{\text{out}}} (h - c\sigma) + (1 - \rho) \mathbb{E}_{P'_{\text{out}}} (h - c\sigma)) \right) \quad (83)$$

The measures are

$$dP_w = \frac{dw e^{\psi_w(w)}}{\int dw e^{\psi_w(w)}} \quad , \quad dP_{\text{out}} = \frac{dh d\sigma e^{\psi_{\text{out}}(h,\sigma;\bar{t}=1)}}{\int dh d\sigma e^{\psi_{\text{out}}(h,\sigma,\bar{t}=1)}} \quad , \quad dP'_{\text{out}} = \frac{dh d\sigma e^{\psi_{\text{out}}(h,\sigma;\bar{t}=0)}}{\int dh d\sigma e^{\psi_{\text{out}}(h,\sigma,\bar{t}=0)}} . \quad (84)$$

These measures can be computed thanks to Laplace's method in the limit  $\beta \rightarrow \infty$ . We have to rescale the order parameters not to obtain a degenerated solution. We recall that  $\log P_W(w) \propto \beta$ . We take  $\hat{V} \rightarrow \beta \hat{V}$ ,  $\hat{Q} \rightarrow \beta^2 \hat{Q}$ ,  $\hat{m} \rightarrow \beta \hat{m}$  and  $V \rightarrow \beta^{-1} V$  for both  $w$  and  $\sigma$ . We define

$$w^* = \operatorname{argmax}_w \psi_w(w) \quad (85)$$

$$(h^*, \sigma^*) = \operatorname{argmax}_{h, \sigma} \psi_{\text{out}}(h, \sigma; \bar{t} = 1) \quad (h'^*, \sigma'^*) = \operatorname{argmax}_{h, \sigma} \psi_{\text{out}}(h, \sigma; \bar{t} = 0); \quad (86)$$

then, keeping the first order in  $\beta$  in both lhs and rhs, the fixed-point equations are

$$m_w = \frac{1}{\alpha} \mathbb{E}_{u, \xi} u w^* \quad m_\sigma = \mathbb{E}_{y, \xi, \zeta, \chi} y \left( \rho \sigma^* + (1 - \rho) \sigma'^* \right) \quad (87)$$

$$Q_w = \frac{1}{\alpha} \mathbb{E}_{u, \xi} (w^*)^2 \quad Q_\sigma = \mathbb{E}_{y, \xi, \zeta, \chi} \left( \rho (\sigma^*)^2 + (1 - \rho) (\sigma'^*)^2 \right) \quad (88)$$

$$V_w = \frac{1}{\alpha} \frac{1}{\sqrt{\hat{Q}_w}} \mathbb{E}_{u, \xi} \xi w^* \quad V_\sigma = \frac{1}{\sqrt{\hat{Q}_\sigma}} \mathbb{E}_{y, \xi, \zeta, \chi} \xi \left( \rho \sigma^* + (1 - \rho) \sigma'^* \right) \quad (89)$$

$$\hat{m}_w = \frac{\sqrt{\mu}}{V_w} \mathbb{E}_{y, \xi, \zeta, \chi} y \left( \rho (\sigma^* - \sqrt{\mu} y m_w) + (1 - \rho) (\sigma'^* - \sqrt{\mu} y m_w) \right) \quad (90)$$

$$\hat{Q}_w = \frac{1}{V_w^2} \mathbb{E}_{y, \xi, \zeta, \chi} \left( \rho (\sigma^* - \sqrt{\mu} y m_w - \sqrt{Q_w} \chi)^2 + (1 - \rho) (\sigma'^* - \sqrt{\mu} y m_w - \sqrt{Q_w} \chi)^2 \right) \quad (91)$$

$$\hat{V}_w = \frac{1}{V_w} \left( 1 - \frac{1}{\sqrt{Q_w}} \mathbb{E}_{y, \xi, \zeta, \chi} \chi \left( \rho \sigma^* + (1 - \rho) \sigma'^* \right) \right) \quad (92)$$

$$\hat{m}_\sigma = \frac{\lambda}{V_\sigma} \mathbb{E}_{y, \xi, \zeta, \chi} y \left( \rho (h^* - c \sigma^* - \lambda y m_\sigma) + (1 - \rho) (h'^* - c \sigma'^* - \lambda y m_\sigma) \right) \quad (93)$$

$$\hat{Q}_\sigma = \frac{1}{V_\sigma^2} \mathbb{E}_{y, \xi, \zeta, \chi} \left( \rho (h^* - c \sigma^* - \lambda y m_\sigma - \sqrt{Q_\sigma} \zeta)^2 + (1 - \rho) (h'^* - c \sigma'^* - \lambda y m_\sigma - \sqrt{Q_\sigma} \zeta)^2 \right) \quad (94)$$

$$\hat{V}_\sigma = \frac{1}{V_\sigma} \left( 1 - \frac{1}{\sqrt{Q_\sigma}} \mathbb{E}_{y, \xi, \zeta, \chi} \zeta \left( \rho (h^* - c \sigma^*) + (1 - \rho) (h'^* - c \sigma'^*) \right) \right) \quad (95)$$

The average train and test losses can be computed by deriving  $\phi$  wrt  $t$  and  $t'$  and taking it extremum by evaluating it at the fixed-point of these equations.

Simplifying the notations we obtain the equations given in the main part.

## A.2 GLM–SBM

Then we derive the results for the GLM–SBM, which has not been studied by [21]. The derivation is similar to the derivation of the previous part on the CSBM. As we showed for the CSBM, one can readily take the test set  $R'$  being the complement of  $R$  i.e.  $\rho' = 1 - \rho$ ; the resulting equations do not change. As stated in eq. (14), we introduce  $n$  replica:

$$\log Z = \frac{\partial}{\partial n} Z^n(n = 0) \quad (96)$$

$$\mathbb{E} Z^n = \mathbb{E}_{u, \Xi, X} \int \underbrace{\prod_a^n \prod_\nu \mathrm{d} w_\nu^a P_W(w_\nu^a) \prod_i \mathrm{d} y_i P_o \left( y_i \mid \frac{1}{\sqrt{N}} X_i^T u \right) e^{\sum_a^n -\beta t \sum_{i \in R} l(y_i h(w^a)_i) - \beta t' \sum_{i \in R'} l(y_i h(w^a)_i)}}_* \quad (97)$$

where  $P_o(y|z) = \delta_{y=\text{sign}(z)}$ . We introduce ancillary variables:  $h = \frac{1}{\sqrt{N}}A\sigma$ ,  $\sigma = \frac{1}{\sqrt{N}}Xw$  and  $z = \frac{1}{\sqrt{N}}Xu$ ; we average over  $\Xi$  and  $X$ , pack the replica and integrate.

$$* \propto \mathbb{E}_{u,\Xi,X} \int \prod_{a,\nu} dw_\nu^a P_W(w_\nu^a) \prod_i dy_i P_o(y_i|z_i) dz_i d\bar{q}_i \prod_{a,i} dh_i^a dq_i^a d\sigma_i^a d\hat{q}_i^a e^{-\beta t \sum_{a,i \in R} l(y_i h_i^a) - \beta t' \sum_{a,i \in R'} l(y_i h_i^a)} e^{\sum_i i\bar{q}_i \left( z_i - \frac{1}{\sqrt{N}} \sum_\nu X_{i\nu} u_\nu \right) + \sum_{a,i} i\bar{q}_i^a \left( h_i^a - \frac{1}{\sqrt{N}} \sum_j \left( c\sqrt{N}\delta_{i,j} + \frac{\lambda}{\sqrt{N}} y_i y_j + \Xi_{ij} \right) \sigma_j^a \right) + \sum_{a,i} i\bar{q}_i^a \left( \sigma_i^a - \frac{1}{\sqrt{N}} \sum_\nu X_{i\nu} w_\nu^a \right)} \quad (98)$$

$$= \mathbb{E}_u \int \prod_{a,\nu} dw_\nu^a P_W(w_\nu^a) \prod_i dy_i P_o(y_i|z_i) dz_i \prod_{a,i} dh_i^a d\sigma_i^a e^{-\beta t \sum_{a,i \in R} l(y_i h_i^a) - \beta t' \sum_{a,i \in R'} l(y_i h_i^a)} \prod_i \mathcal{N} \left( h_i \left| c\sigma_i + \frac{\lambda}{N} y_i \sum_j y_j \sigma_j, \frac{1}{N} \sum_j \sigma_j \sigma_j^T \right. \right) \prod_i \mathcal{N} \left( \left( \begin{array}{c} z_i \\ \sigma_i \end{array} \right) \left| 0, \frac{1}{N} \sum_\nu \left( \begin{array}{c} u_\nu \\ w_\nu \end{array} \right) \left( \begin{array}{c} u_\nu \\ w_\nu \end{array} \right)^T \right. \right). \quad (99)$$

Here  $\left( \begin{array}{c} z_i \\ \sigma_i \end{array} \right)$  and  $\left( \begin{array}{c} u_\nu \\ w_\nu \end{array} \right)$  are vectors of size  $n+1$ .  $\frac{1}{N} \sum_\nu u_\nu^2$  self-averages to  $\rho_u := \frac{1}{\alpha} \mathbb{E}_u u^2 = \frac{1}{\alpha}$ . We introduce the order parameters :

$$* \propto \mathbb{E}_u \int \prod_{a,\nu} dw_\nu^a P_W(w_\nu^a) \prod_i dy_i P_o(y_i|z_i) dz_i \prod_{a,i} dh_i^a d\sigma_i^a \prod_{a \leq b} d\hat{Q}_w^{ab} dQ_w^{ab} d\hat{Q}_\sigma^{ab} dQ_\sigma^{ab} \prod_a d\hat{m}_w^a dm_w^a d\hat{m}_\sigma^a dm_\sigma^a \quad (100)$$

$$\prod_{a \leq b} e^{\hat{Q}_w^{ab} (NQ_w^{ab} - \sum_\nu w_\nu^a w_\nu^b) + \hat{Q}_\sigma^{ab} (NQ_\sigma^{ab} - \sum_i \sigma_i^a \sigma_i^b)} \prod_a e^{\hat{m}_w^a (Nm_w^a - \sum_\nu u_\nu w_\nu^a) + \hat{m}_\sigma^a (Nm_\sigma^a - \sum_i y_i \sigma_i^a)} e^{-\beta t \sum_{a,i \in R} l(y_i h_i^a) - \beta t' \sum_{a,i \in R'} l(y_i h_i^a)} \prod_i N(h_i | c\sigma_i + \lambda y_i m_\sigma, Q_\sigma) \mathcal{N} \left( \left( \begin{array}{c} z_i \\ \sigma_i \end{array} \right) \left| 0, \left( \begin{array}{cc} \rho_u & m_w^T \\ m_w & Q_w \end{array} \right) \right. \right) = \int \prod_{a \leq b} d\hat{Q}_w^{ab} dQ_w^{ab} d\hat{Q}_\sigma^{ab} dQ_\sigma^{ab} \prod_a dm_w^a d\hat{m}_w^a dm_\sigma^a d\hat{m}_\sigma^a \prod_{a \leq b} e^{N(\hat{Q}_w^{ab} Q_w^{ab} + \hat{Q}_\sigma^{ab} Q_\sigma^{ab})} \prod_a e^{N(\hat{m}_w^a m_w^a + \hat{m}_\sigma^a m_\sigma^a)} \quad (101)$$

$$\left[ \mathbb{E}_u \int \prod_a dw^a e^{\psi_w^{(n)}(w)} \right]^{N/\alpha} \left[ \int dy P_o(y|z) dz \prod_a dh^a d\sigma^a e^{\psi_{\text{out}}^{(n)}(h,\sigma;t)} \right]^{\rho N} \left[ \int dy P_o(y|z) dz \prod_a dh^a d\sigma^a e^{\psi_{\text{out}}^{(n)}(h,\sigma;t')} \right]^{(1-\rho)N};$$

where we defined

$$\psi_w^{(n)}(w) = \sum_a \log P_W(w^a) - \sum_{a \leq b} \hat{Q}_w^{ab} w^a w^b - \sum_a \hat{m}_w^a u w^a \quad (102)$$

$$\psi_{\text{out}}^{(n)}(h, \sigma; \bar{t}) = -\beta \bar{t} \sum_a l(yh^a) - \sum_{a \leq b} \hat{Q}_\sigma^{ab} \sigma^a \sigma^b - \sum_a \hat{m}_\sigma^a y \sigma^a - \frac{1}{2} (h - c\sigma - \lambda y m_\sigma)^T Q_\sigma^{-1} (h - c\sigma - \lambda y m_\sigma) - \frac{1}{2} \log \det Q_\sigma - \frac{1}{2} \left( \begin{array}{c} z \\ \sigma \end{array} \right)^T \left( \begin{array}{cc} \rho_u & m_w^T \\ m_w & Q_w \end{array} \right)^{-1} \left( \begin{array}{c} z \\ \sigma \end{array} \right) - \frac{1}{2} \log \det \left( \begin{array}{cc} \rho_u & m_w^T \\ m_w & Q_w \end{array} \right). \quad (103)$$

We use the replica-symmetric ansatz: we set  $\hat{Q}^{aa} = \frac{1}{2}\hat{R}$ ,  $\hat{Q}^{ab} = -\hat{Q}$ ,  $Q^{aa} = R$ ,  $Q^{ab} = Q$ ,  $\hat{m}^a = -\hat{m}$  and  $m^a = m$ . We define the variances  $V = R - Q$  and  $\hat{V} = \hat{R} + \hat{Q}$ . We take the first order in  $n$ ; and as before we have

$$Q_\sigma^{-1} = \frac{1}{V_\sigma} I_n - \frac{Q_\sigma}{V_\sigma^2} J_{n,n} + o(n) \quad (104)$$

$$\log \det Q_\sigma = n \frac{Q_\sigma}{V_\sigma} + n \log(V_\sigma) + o(n); \quad (105)$$

we compute that

$$\begin{pmatrix} \rho_u & m_w^T \\ m_w & Q_w \end{pmatrix}^{-1} = \begin{pmatrix} \frac{1}{\rho_u} + n \frac{m_w^2}{V_w \rho_u^2} & -\frac{m_w}{V_w \rho_u} (1, \dots, 1) \\ -\frac{m_w}{V_w \rho_u} (1, \dots, 1)^T & \frac{1}{V_w} I_n - \frac{1}{V_w^2} (Q_w - \frac{m_w^2}{\rho_u}) J_{n,n} \end{pmatrix} \quad (106)$$

$$\log \det \begin{pmatrix} \rho_u & m_w^T \\ m_w & Q_w \end{pmatrix} = \log \rho_u + \frac{n}{V_w} (Q_w - \frac{m_w^2}{\rho_u}) + n \log V_w + o(n) . \quad (107)$$

We can factorize the replica introducing scalar standard Gaussians:

$$\begin{aligned} * \propto & \int d\hat{Q}_w d\hat{V}_w dQ_w dV_w d\hat{Q}_\sigma d\hat{V}_\sigma dQ_\sigma dV_\sigma d\hat{m}_w dm_w d\hat{m}_\sigma dm_\sigma e^{\frac{nN}{2} (\hat{V}_w V_w + \hat{V}_w Q_w - V_w \hat{Q}_w + \hat{V}_\sigma V_\sigma + \hat{V}_\sigma Q_\sigma - V_\sigma \hat{Q}_\sigma)} \\ & e^{-nN(\hat{m}_w m_w + \hat{m}_\sigma m_\sigma)} \left[ \mathbb{E}_{u,\xi} \left( \int dw e^{\psi_w(w)} \right)^n \right]^{N/\alpha} \left[ \mathbb{E}_{\xi,\zeta,\chi} \int dy dz \psi_{\text{out}}^*(y, z) \left( \int dh d\sigma e^{\psi_{\text{out}}(h, \sigma; t)} \right)^n \right]^{\rho N} \\ & \left[ \mathbb{E}_{\xi,\zeta,\chi} \int dy dz \psi_{\text{out}}^*(y, z) \left( \int dh d\sigma e^{\psi_{\text{out}}(h, \sigma; t)} \right)^n \right]^{(1-\rho)N} ; \end{aligned} \quad (108)$$

with

$$\psi_w(w) = \log P_W(w) - \frac{1}{2} \hat{V}_w w^2 + \left( \xi \sqrt{\hat{Q}_w} + u \hat{m}_w \right) w \quad (109)$$

$$\psi_{\text{out}}(h, \sigma; \bar{t}) = -\beta \bar{t} l(yh) - \frac{1}{2} \hat{V}_\sigma \sigma^2 + \left( \xi \sqrt{\hat{Q}_\sigma} + y \hat{m}_\sigma \right) \sigma \quad (110)$$

$$+ \log \mathcal{N} \left( h | c\sigma + \lambda y m_\sigma + \sqrt{Q_\sigma} \zeta, V_\sigma \right) + \log \mathcal{N} \left( \sigma | \rho_u^{-1} m_w z + \sqrt{(1 - \eta_w) Q_w} \chi, V_w \right) \quad (111)$$

$$\psi_{\text{out}}^*(y, z) = P_o(y|z) \mathcal{N}(z|0, \rho_u) ,$$

where we defined  $\eta_w = \frac{m_w^2}{\rho_u Q_w}$ . We take the limit  $N \rightarrow \infty$  and  $n \rightarrow 0$ . The free entropy is then

$$\begin{aligned} \phi = & \frac{1}{2} \left( \hat{V}_w V_w + \hat{V}_w Q_w - V_w \hat{Q}_w + \hat{V}_\sigma V_\sigma + \hat{V}_\sigma Q_\sigma - V_\sigma \hat{Q}_\sigma \right) - \hat{m}_w m_w - \hat{m}_\sigma m_\sigma + \frac{1}{\alpha} \mathbb{E}_{u,\xi} \left( \log \int dw e^{\psi_w(w)} \right) \\ & + \rho \mathbb{E}_{\xi,\zeta,\chi} \left( \int dy dz \psi_{\text{out}}^*(y, z) \log \int dh d\sigma e^{\psi_{\text{out}}(h, \sigma; t)} \right) \\ & + (1 - \rho) \mathbb{E}_{\xi,\zeta,\chi} \left( \int dy dz \psi_{\text{out}}^*(y, z) \log \int dh d\sigma e^{\psi_{\text{out}}(h, \sigma; t')} \right) . \end{aligned} \quad (112)$$

As before we rescale the order parameters according to  $\hat{V} \rightarrow \beta \hat{V}$ ,  $\hat{Q} \rightarrow \beta^2 \hat{Q}$ ,  $\hat{m} \rightarrow \beta \hat{m}$  and  $V \rightarrow \beta^{-1} V$  for both  $w$  and  $\sigma$ , so in the limit  $\beta \rightarrow \infty$  by Laplace's method the inner integrals are not degenerated. We define

$$w^* = \underset{w}{\text{argmax}} \psi_w(w) \quad (113)$$

$$(h^*, \sigma^*) = \underset{h, \sigma}{\text{argmax}} \psi_{\text{out}}(h, \sigma; \bar{t} = 1) \quad (h'^*, \sigma'^*) = \underset{h, \sigma}{\text{argmax}} \psi_{\text{out}}(h, \sigma; \bar{t} = 0) . \quad (114)$$

The fixed-point equations are

$$m_w = \frac{1}{\alpha} \mathbb{E}_{u,\xi} u w^* \quad m_\sigma = \mathbb{E}_{\xi,\zeta,\chi} \int dy dz \psi_{\text{out}}^*(y, z) y \left( \rho \sigma^* + (1 - \rho) \sigma'^* \right) \quad (115)$$

$$Q_w = \frac{1}{\alpha} \mathbb{E}_{u,\xi} (w^*)^2 \quad Q_\sigma = \mathbb{E}_{\xi,\zeta,\chi} \int dy dz \psi_{\text{out}}^*(y, z) \left( \rho (\sigma^*)^2 + (1 - \rho) (\sigma'^*)^2 \right) \quad (116)$$

$$V_w = \frac{1}{\alpha} \frac{1}{\sqrt{\hat{Q}_w}} \mathbb{E}_{u,\xi} \xi w^* \quad V_\sigma = \frac{1}{\sqrt{\hat{Q}_\sigma}} \mathbb{E}_{\xi,\zeta,\chi} \int dy dz \psi_{\text{out}}^*(y, z) \xi \left( \rho \sigma^* + (1 - \rho) \sigma'^* \right) \quad (117)$$

$$\hat{m}_w = \frac{1}{V_w} \mathbb{E}_{\xi, \zeta, \chi} \int dy dz \psi_{\text{out}}^*(y, z) \left( \rho_u^{-1} z - \chi \frac{\rho_u^{-1} m_w}{\sqrt{(1 - \eta_w) Q_w}} \right) (\rho \sigma^* + (1 - \rho) \sigma'^*) \quad (118)$$

$$\begin{aligned} \hat{Q}_w &= \frac{1}{V_w^2} \mathbb{E}_{\xi, \zeta, \chi} \int dy dz \psi_{\text{out}}^*(y, z) \left( \rho (\sigma^* - \rho_u^{-1} m_w z - \chi \sqrt{(1 - \eta_w) Q_w})^2 \right. \\ &\quad \left. + (1 - \rho) (\sigma'^* - \rho_u^{-1} m_w z - \chi \sqrt{(1 - \eta_w) Q_w})^2 \right) \end{aligned} \quad (119)$$

$$\hat{V}_w = \frac{1}{V_w} \left( 1 - \frac{1}{\sqrt{(1 - \eta_w) Q_w}} \mathbb{E}_{\xi, \zeta, \chi} \int dy dz \psi_{\text{out}}^*(y, z) \chi (\rho \sigma^* + (1 - \rho) \sigma'^*) \right) \quad (120)$$

$$\hat{m}_\sigma = \frac{\lambda}{V_\sigma} \mathbb{E}_{\xi, \zeta, \chi} \int dy dz \psi_{\text{out}}^*(y, z) y \left( \rho (h^* - c \sigma^* - \lambda y m_\sigma) + (1 - \rho) (h'^* - c \sigma'^* - \lambda y m_\sigma) \right) \quad (121)$$

$$\begin{aligned} \hat{Q}_\sigma &= \frac{1}{V_\sigma^2} \mathbb{E}_{\xi, \zeta, \chi} \int dy dz \psi_{\text{out}}^*(y, z) \left( \rho (h^* - c \sigma^* - \lambda y m_\sigma - \sqrt{Q_\sigma} \zeta)^2 + (1 - \rho) (h'^* - c \sigma'^* - \lambda y m_\sigma - \sqrt{Q_\sigma} \zeta)^2 \right) \\ &\quad (122) \end{aligned}$$

$$\hat{V}_\sigma = \frac{1}{V_\sigma} \left( 1 - \frac{1}{\sqrt{Q_\sigma}} \mathbb{E}_{\xi, \zeta, \chi} \int dy dz \psi_{\text{out}}^*(y, z) \zeta (\rho (h^* - c \sigma^*) + (1 - \rho) (h'^* - c \sigma'^*)) \right) \quad (123)$$

The average train and test losses can be computed by deriving  $\phi$  wrt  $t$  and  $t'$  and taking it extremum by evaluating it at the fixed-point of these equations.

The integral on  $z$  can be computed by the change of variable  $\chi \rightarrow \frac{\chi}{\sqrt{1 - \eta_w}} - \frac{\rho_u^{-1} m_w z}{\sqrt{(1 - \eta_w) Q_w}}$ . We obtain the expressions given in the main part, after simplification of the notations.

### A.3 Ridge-regression

We derive the simplified fixed-point equations that allow to compute the learning rates of the GCN stated in section 4.2. For  $l_2$ -regularization, quadratic loss and no self-loops  $c = 0$  the two above systems of fixed-point equations are equivalent to two simpler ones. For the CSBM it reads

$$Q_w = \frac{1}{\alpha} \frac{\hat{Q}_w + \hat{m}_w^2}{(r + \hat{V}_w)^2} \quad V_w = \frac{1}{\alpha} \frac{1}{r + \hat{V}_w} \quad m_w = \frac{1}{\alpha} \frac{\hat{m}_w}{r + \hat{V}_w} \quad (124)$$

$$Q_\sigma = V_w^2 \frac{\hat{Q}_\sigma + (\hat{m}_\sigma + \sqrt{\mu} \frac{m_w}{V_w})^2 + \frac{Q_w}{V_w^2}}{(1 + V_w \hat{V}_\sigma)^2} \quad V_\sigma = \frac{V_w}{1 + V_w \hat{V}_\sigma} \quad m_\sigma = \frac{V_w}{1 + V_w \hat{V}_\sigma} \left( \hat{m}_\sigma + \sqrt{\mu} \frac{m_w}{V_w} \right) \quad (125)$$

$$\hat{Q}_w = \frac{\hat{Q}_\sigma + (\hat{m}_\sigma - \sqrt{\mu} \hat{V}_\sigma m_w)^2 + \hat{V}_\sigma^2 Q_w}{(1 + V_w \hat{V}_\sigma)^2} \quad \hat{V}_w = \frac{\hat{V}_\sigma}{1 + V_w \hat{V}_\sigma} \quad \hat{m}_w = \sqrt{\mu} \frac{1}{1 + V_w \hat{V}_\sigma} (\hat{m}_\sigma - \sqrt{\mu} \hat{V}_\sigma m_w) \quad (126)$$

$$\hat{Q}_\sigma = \rho \frac{Q_\sigma + (1 - \lambda m_\sigma)^2}{(1 + V_\sigma)^2} \quad \hat{V}_\sigma = \frac{\rho}{1 + V_\sigma} \quad \hat{m}_\sigma = \lambda \frac{\rho}{1 + V_\sigma} (1 - \lambda m_\sigma) \quad (127)$$

and for the GLM–SBM it reads

$$Q_w = \frac{1}{\alpha} \frac{\hat{Q}_w + \hat{m}_w^2}{(r + \hat{V}_w)^2} \quad V_w = \frac{1}{\alpha} \frac{1}{r + \hat{V}_w} \quad m_w = \frac{1}{\alpha} \frac{\hat{m}_w}{r + \hat{V}_w} \quad (128)$$

$$Q_\sigma = V_w^2 \frac{\hat{Q}_\sigma + (\hat{m}_\sigma + \sqrt{\frac{2}{\pi \rho_u}} \frac{m_w}{V_w})^2 + (1 - \frac{2}{\pi} \eta_w) \frac{Q_w}{V_w^2}}{(1 + V_w \hat{V}_\sigma)^2} \quad V_\sigma = \frac{V_w}{1 + V_w \hat{V}_\sigma} \quad m_\sigma = \frac{V_w}{1 + V_w \hat{V}_\sigma} \left( \hat{m}_\sigma + \sqrt{\frac{2}{\pi \rho_u}} \frac{m_w}{V_w} \right) \quad (129)$$

$$\hat{Q}_w = \frac{\hat{Q}_\sigma + (\hat{m}_\sigma - \sqrt{\frac{2}{\pi \rho_u}} \hat{V}_\sigma m_w)^2 + (1 - \frac{2}{\pi} \eta_w) \hat{V}_\sigma^2 Q_w}{(1 + V_w \hat{V}_\sigma)^2} \quad \hat{V}_w = \frac{\hat{V}_\sigma}{1 + V_w \hat{V}_\sigma} \quad \hat{m}_w = \sqrt{\frac{2}{\pi \rho_u}} \frac{1}{1 + V_w \hat{V}_\sigma} \hat{m}_\sigma \quad (130)$$

$$\hat{Q}_\sigma = \rho \frac{Q_\sigma + (1 - \lambda m_\sigma)^2}{(1 + V_\sigma)^2} \quad \hat{V}_\sigma = \frac{\rho}{1 + V_\sigma} \quad \hat{m}_\sigma = \lambda \frac{\rho}{1 + V_\sigma} (1 - \lambda m_\sigma) \quad (131)$$

where  $\rho_u = \alpha^{-1}$  and  $\eta_w = \frac{m_w^2}{\rho_u Q_w}$ . For the two models the losses and accuracies are

$$E_{\text{train}} = \frac{1}{2\rho} \hat{Q}_\sigma \quad E_{\text{test}} = \frac{1}{2\rho} (1 + V_\sigma)^2 \hat{Q}_\sigma \quad (132)$$

$$\text{Acc}_{\text{train}} = \frac{1}{2} \left( 1 + \text{erf} \left( \frac{V_\sigma + \lambda m_\sigma}{\sqrt{2} Q_\sigma} \right) \right) \quad \text{Acc}_{\text{test}} = \frac{1}{2} \left( 1 + \text{erf} \left( \frac{\lambda m_\sigma}{\sqrt{2} Q_\sigma} \right) \right) . \quad (133)$$

## B Bayes-optimal performances

In section 4 we compare the GCN to the Bayes-optimal performances. The Bayes-optimal performances on the CSBM and the GLM–SBM were derived by [10] and [2, 9]. They can be expressed as a function of the fixed-point of a system of equations over three scalar quantities.

These works consider a SBM with symmetric fluctuations  $\Xi$  in the adjacency matrix  $A = \frac{\lambda}{\sqrt{N}} yy^T + \Xi$ . In our work for simplicity we take  $\Xi$  non-symmetric. Then the corresponding  $A$  can be mapped to the matrix of a symmetric SBM by the transform  $(A + A^T)/\sqrt{2}$  and it is sufficient to rescale the snr  $\lambda$  of the symmetric SBM by  $\sqrt{2}$  to have the same snr as for the non-symmetric SBM. So we set  $\Delta_I = 2\lambda^2$  the signal-to-noise ratio of the corresponding low-rank matrix factorization problem.

### B.1 CSBM

The equations are given by [10] in its appendix. The self-consistent equations read

$$m^t = \frac{\mu}{\alpha} m_u^t + \Delta_I m_y^{t-1} \quad (134)$$

$$m_y^t = \rho + (1 - \rho) \mathbb{E}_W \left[ \tanh \left( m^t + \sqrt{m^t} W \right) \right] \quad (135)$$

$$m_u^{t+1} = \frac{\mu m_y^t}{1 + \mu m_y^t} \quad (136)$$

where  $W$  is a standard scalar Gaussian. Once a fixed-point  $(m, m_y, m_u)$  is obtained the test accuracy is given by

$$\text{Acc}_{\text{test}} = \frac{1}{2} (1 + \text{erf} \sqrt{m/2}) . \quad (137)$$

In the large  $\lambda$  limit we have  $m_y \rightarrow 1$  and

$$\text{Acc}_{\text{test}} \xrightarrow{\lambda \rightarrow \infty} \frac{1}{2} (1 + \text{erf} \lambda) . \quad (138)$$

### B.2 GLM–SBM

The equations are given by [2], only for the unsupervised case  $\rho = 0$ . The supervised part can be inferred from the simpler case of Bayes-optimal inference on a GLM [5]. Then the supervised part and the unsupervised part are merged in a linear fashion as on the CSBM. We need the following (not normalized) density on  $y$  and  $z$ :

$$Q(y, z; B, A, \omega, V) = P_o(y|z) e^{-A/2 + B y} \frac{e^{-(z-\omega)^2/2V}}{\sqrt{2\pi V}} . \quad (139)$$

We define the update functions

$$Z_{\text{out}}(B, A, \omega, V) = \int dy dz Q(y, z; B, A, \omega, V) \quad Z_{\text{out}}^{\text{sup}}(\omega, V) = \int dz Q(+1, z; 0, 0, \omega, V) \quad (140)$$

$$= e^{-A/2} \left( \cosh B + \sinh(B) \text{erf}(\omega/\sqrt{2V}) \right) \quad = \frac{1}{2} \left( 1 + \text{erf}(\omega/\sqrt{2V}) \right) \quad (141)$$

$$f_{\text{out}} = \partial_\omega \log Z_{\text{out}} \quad f_{\text{out}}^{\text{sup}} = \partial_\omega \log Z_{\text{out}}^{\text{sup}} \quad (142)$$

$$f_y = \partial_B \log Z_{\text{out}} \quad (143)$$

Then the self-consistent equations read

$$\hat{m}_u^t = \rho \mathbb{E}_\eta \left[ Z_{\text{out}}^{\sup} \left( \sqrt{m_u^t} \eta, \rho_u - m_u^t \right) f_{\text{out}}^{\sup} \left( \sqrt{m_u^t} \eta, \rho_u - m_u^t \right)^2 \right] \quad (144)$$

$$\begin{aligned} & + (1 - \rho) \mathbb{E}_{\xi, \eta} \left[ Z_{\text{out}} \left( \sqrt{\Delta_I m_y^t} \xi, \Delta_I m_y^t, \sqrt{m_u^t} \eta, \rho_u - m_u^t \right) f_{\text{out}} \left( \sqrt{\Delta_I m_y^t} \xi, \Delta_I m_y^t, \sqrt{m_u^t} \eta, \rho_u - m_u^t \right)^2 \right] \\ m_y^{t+1} & = \rho + (1 - \rho) \mathbb{E}_{\xi, \eta} \left[ Z_{\text{out}} \left( \sqrt{\Delta_I m_y^t} \xi, \Delta_I m_y^t, \sqrt{m_u^t} \eta, \rho_u - m_u^t \right) f_y \left( \sqrt{\Delta_I m_y^t} \xi, \Delta_I m_y^t, \sqrt{m_u^t} \eta, \rho_u - m_u^t \right)^2 \right] \end{aligned} \quad (145)$$

$$m_u^{t+1} = \frac{1}{\alpha} \frac{\hat{m}_u^t}{1 + \hat{m}_u^t} \quad (146)$$

where  $\xi$  and  $\eta$  are standard scalar Gaussians and  $\rho_u = \alpha^{-1}$ . Once a fixed-point  $(\hat{m}_u, m_y, m_u)$  is obtained the test accuracy is given by

$$\text{Acc}_{\text{test}} = \mathbb{E}_{\xi, \eta} \left[ \int dy dz Q \left( y, z; \sqrt{\Delta_I m_y} \xi, \Delta_I m_y, \sqrt{m_u} \eta, \rho_u - m_u \right) \delta_{y=\text{sign } f_y(\sqrt{\Delta_I m_y} \xi, \Delta_I m_y, \sqrt{m_u} \eta, \rho_u - m_u)} \right] \quad (147)$$

$$= \mathbb{E}_\eta \left[ \frac{1}{2} \left( 1 + \text{erf} \left( \frac{\sqrt{m_u} \eta}{\sqrt{2}(\rho_u - m_u)} \right) \right) \left( 1 + \text{erf} \left( \frac{\sqrt{\Delta_I m_y}}{\sqrt{2}} + \frac{1}{\sqrt{2\Delta_I m_y}} \text{arcth} \text{erf} \left( \frac{\sqrt{m_u} \eta}{\sqrt{2}(\rho_u - m_u)} \right) \right) \right) \right]. \quad (148)$$

In the large  $\lambda$  limit we have  $m_y \rightarrow 1$  and

$$\text{Acc}_{\text{test}} \xrightarrow{\lambda \rightarrow \infty} \frac{1}{2} (1 + \text{erf} \lambda). \quad (149)$$

## C Details on numeric

The systems (22)-(30) and (34)-(42) are solved by the iterating the twelve equations in parallel until convergence. About twenty iterations are necessary. The iterations are stable and no damping is necessary. The integral over  $(\xi, \zeta, \chi)$  is evaluated by Monte-Carlo over  $10^6$  points; we use the same samples over the iterations so they can exactly converge. For the quadratic and hinge losses the extremizer of the potential 17 has an explicit solution; for the logistic loss we compute it by Newton's descent, a few steps are enough. The whole computation takes around one minute on a single CPU core with 5GB of memory.

For figures 3 and 4 solving these two systems we were only able to reach misclassification errors  $1 - \text{Acc}_{\text{test}}$  of  $10^{-6}$  because of numerical imprecision and the finite number of Monte-Carlo samples.

## D Supplementary figures

On Fig. 5 we show that an interpolation peak appears for the logistic regression on the CSBM when the regularization is small while varying the training ratio  $\rho$ . At the interpolation peak the train error becomes strictly positive, the train accuracy becomes strictly smaller than one, the test error diverges and the test accuracy has an inflexion point. The position of the peak depends on the self-loop intensity  $c$  and the aspect ratio  $\alpha$ . Increasing the regularization  $r$  smooths it out. Similar curves are obtained for the hinge loss and the GLM–SBM.

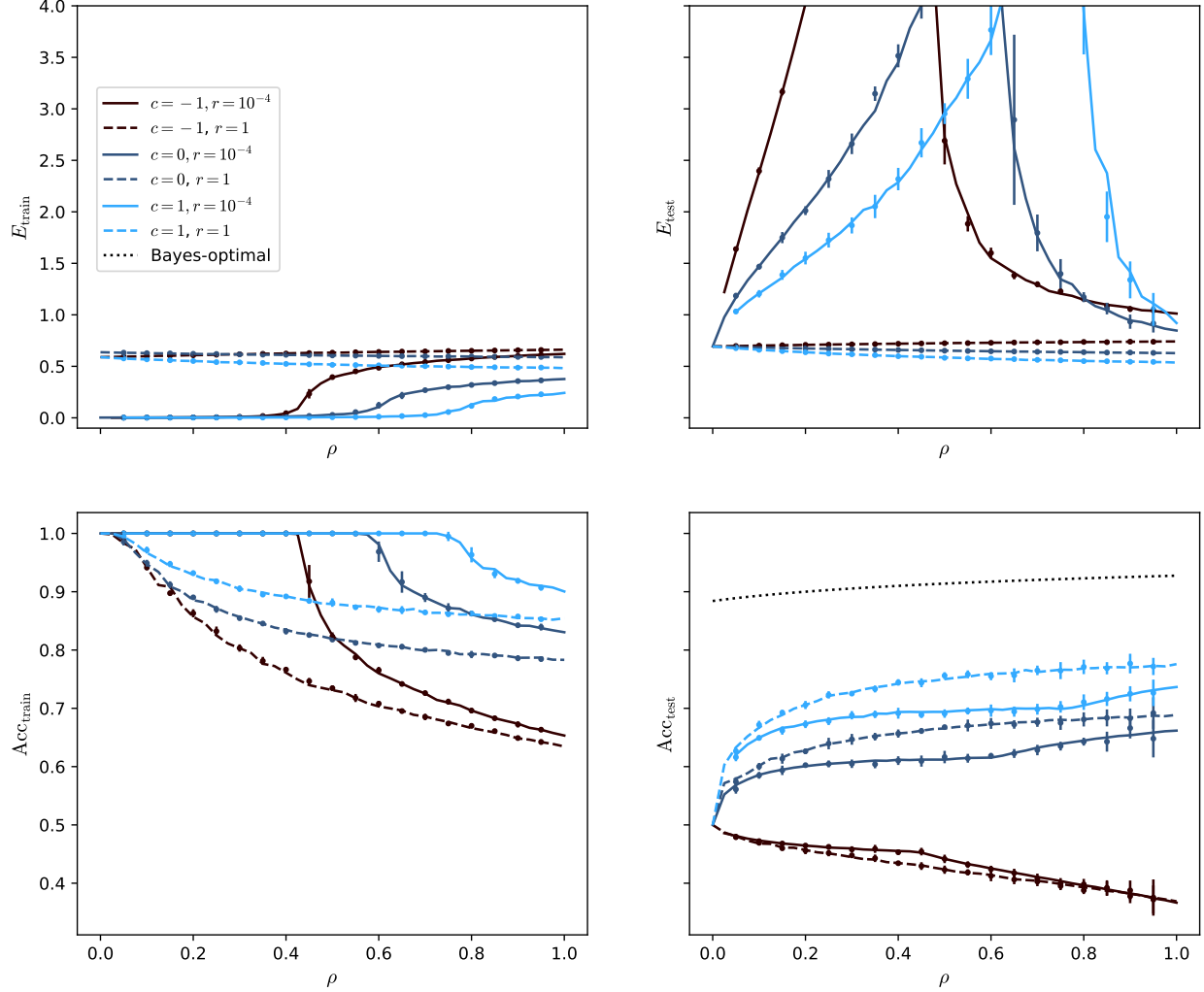


Figure 5: Interpolation peak on the CSBM for the logistic loss.  $\alpha = 4$ ,  $\lambda = 1$  and  $\mu = 1$ . Lines: predictions by (22)-(32); dots: numerical simulation of the GCN for  $N = 10^4$  and  $d = N/2$ , averaged over ten experiments; dotted line: Bayes-optimal test accuracy.